

國立臺灣大學工學院化學工程學研究所

碩士論文

Department of Chemical Engineering

College of Engineering

National Taiwan University

Master Thesis

利用具有自組裝能力之兩性高分子及奈米粒子混參

材料製作軟性仿生透鏡

**Bionic Soft Lens Materials Based on Self-Assembling
Amphiphilic Block Copolomer/Nanoparticle Hybrids**



陳建鈞

Chien-Chun Chen

指導教授：戴子安 博士

Advisor: Chi-An Dai, Ph.D.

中華民國 99 年 7 月

July, 2010

誌謝

經過兩年的學習與歷練，本論文終於順利完成，首先要感謝指導教授戴子安博士授與專業知識以及思考上的啟發，還要感謝口試委員何國川博士、施文彬博士、吳嘉文博士、張家華博士於論文口試中提出學生論文上的指導以及提供寶貴的建議，在此深深地感謝。

在研究過程中承蒙台大醫院王一中醫師提供實驗室之設備及實驗中的寶貴建議。另外感謝宜桓學長、鈞傑學長、宜龍學長、育凭學長、奇儒學長、以及士鈞學長，播空出來協助學生之研究及指導，使本論文能夠更加完善。

另外，實驗室一起奮鬥的夥伴智中、崇文、豐瑜、傑荃，感謝你們的幫忙以及鼓勵，一起渡過實驗中的困境及一起分享實驗成果的喜悅。也感謝實驗室凡凱、孟弘、怡辰、泓瑋學弟的幫忙，有了你們，在研究所生涯能更加踏實，在此由衷的謝謝大家，也祝福你們。

最後要感謝我的父母，感謝你們在研究所生涯中的鼓勵與關懷，不管在物質或精神上面都很充實，可以無後顧之憂的順利完成學業。

這篇論文獻給研究所生涯中，所認識的每一個人，願大家都能平安、快樂！

陳建鈞 2010/07/21

中文摘要

此篇論文中揭示了一種注入型水晶體材料的開發與光學性質之量測。本實驗以尾端改質且具熱敏感性之泊洛沙姆(Poloxamer)高分子為主體，藉由光起始作用進行交聯，以形成人工水晶體材料。泊洛沙姆之尾端氫氧官能基經由丙烯酰氯反應而形成具有丙烯酸官能基高分子，並經由核磁共振(NMR)及紅外光吸收光譜(FTIR)確認。由於泊洛沙姆高分子具有溶液-凝膠轉變的現象，而凝膠狀態可以防止材料注入水晶體時所造成的滲漏現象。改質過後的泊洛沙姆高分子其溶液-凝膠轉變溫度在濃度低於 20%時高於未改質之泊洛沙姆高分子，但濃度若高於 22%時則兩者表現幾乎相同。經由光起始交聯的泊洛沙姆水膠的楊氏係數會隨著水膠中未改質的泊洛沙姆高分子比例的增加或紫外光起始時間的減少，其楊氏係數會由 230kPa 降低到 18kPa，但光起始劑濃度的影響卻不明顯。

為了增加泊洛沙姆水膠的折射度以符合水晶體需求，在水膠中加入利用四氯化鈦為原料所製作出的奈米二氧化鈦粒子。四氯化鈦經由水解、中和、沈澱、過濾及膠解的過程，可以做出分散在水溶液狀態下的奈米二氧化鈦粒子溶液。根據泊洛沙姆水膠中奈米二氧化鈦粒子濃度的增加，折射率會從原本的 1.355 提升至 1.407，且含有奈米二氧化鈦粒子之泊洛沙姆水膠在可見光範圍皆有良好的穿透度 (~90%)，約略等於人類 5 歲時水晶體的穿透度。

在變焦實驗中，填入高折射率的泊洛沙姆水膠水晶體囊袋其焦距變化(2.53D)比填入低折射率的水晶體囊袋變化(0.87D)來的大，但平均變焦比例幾乎相同(16.57%)，且皆高於人體水晶體(8.37%)。

此論文中也利用電場擴散的方法來模擬人體水晶體中的折射梯度結構的製作。實

驗結果證明，利用電場法在低電場強度時即可使奈米二氧化鈦粒子以輻射的方式進行擴散，形成折射梯度之結構。最後藉由光起始交聯的網狀結構使奈米二氧化鈦粒子被固定在泊洛沙姆水膠中，使具有折射梯度之結構被固定。實驗結果也可看出折射梯度的形成能夠提升透鏡成像之品質。利用以上之實驗結果，我們研發出一種有機/無機混合之新穎性材料，對於人工水晶體之研發具有相當之潛力。

關鍵字：泊洛沙姆水膠，溶液-凝膠，奈米二氧化鈦粒子，折射梯度，可注射式材料



Abstract

In this study, the potentiality to investigate hydrogel which can be injected into crystalline lens is studied. Hydrogel base on thermo-sensitive poloxamer 407 block copolymer is prepared by photo-polymerization. The terminal hydroxyl groups in poloxamer 407 are acrylated to form poloxamer 407 macromer as the reactive polymer, and is confirmed using NMR and FTIR spectrometry. The lower critical sol-gel temperature of poloxamer 407 macromer is higher than poloxamer 407 itself when the concentration is below 20%, but not significant above 22%. The Young's modulus would be decreased according to the higher ratio of poloxamer 407 that in poloxamer hydrogel or shorter UV irradiation times, but the concentration of photo initiator is not significant.

In order to increase the refractive index of poloxamer hydrogel, titanium dioxide nanoparticle is introduced using the titanium (IV) chloride as titanium source. Titanium chloride through the process of hydrolysis, adjust pH, precipitate and acid-peptization can get the rutile phase titanium dioxide nanoparticles solution. The refractive index of poloxamer hydrogel can increase from 1.355 to 1.407 according to the concentration of titanium dioxide nanoparticles, and all samples had a good transmission (~90%) comparable to a 5-year-old natural crystalline lens.

Stretch and unstretch experiment shows the PDMS capsule which filled with the highest refractive index poloxamer hydrogel has the largest change of diopter (2.53D), and the lowest refractive index poloxamer hydrogel shows the smallest change (0.87D). The average change ability is 16.57%, better than the human crystalline lens, about 8.37%.

The gradient refractive index structure in the human crystalline lens also

reconstruct by using the electric field method. The distribution of titanium dioxide nanoparticles can be controlled by electric field in poloxamer hydrogel, which presents the radial gradient refractive index profiles. Finally we cross-linked poloxamer hydrogel that the gradient refractive index structure can be maintained. The experiment data also show the gradient refractive index does have the ability to increase the image quality. The novel organic/inorganic hybrid materials show the potential to be used for crystalline lens applications.

Keyword : poloxamer hydrogel, lower critical sol-gel temperature, titanium dioxide nanoparticles, gradient refractive index, injectable materials



Table of Contents

誌謝	I
中文摘要	II
Abstract	IV
Table of Contents	VI
List of Figures	VIII
List of Tables	XI
Chapter 1 Introduction	1
Chapter 2 Paper review	3
2.1. Injectable materials	3
2.1.1. Silicon gelation	4
2.1.2. Hydrogel	5
2.1.2.1. Pluronic tri-block-co-polymers	6
2.1.3. Polyurethane	7
2.1.4. Disulfide gelation	7
2.2. The high refractive index materials	8
2.2.1 Titanium dioxide	8
2.3. Gradient refractive index (GRIN) structure	10
Chapter 3 Experiment	13
3.1. Experiment materials	13
3.2. Experiment Instruments	14
3.3. Experimental Procedure	16
3.4. Experiment Methods	17
3.4.1. Modification of the terminal groups of poloxamer 407	17

3.4.2. The lower critical sol-gel temperature of poloxamer hydrogel	18
3.4.3. The mechanism property of poloxamer hydrogel.....	19
3.4.4. Preparing the titanium dioxide nanoparticles	20
3.4.5. Refractive index of poloxamer/titanium dioxide nanoparticles hybrids	21
3.4.6. Measuring the focal length based on PDMS capsule	22
3.4.7. Reconstruct the 1-dimension gradient refractive index structure.....	23
3.4.7.1. The Fick’s law diffusion method	23
3.4.7.2. The centrifuged method.....	23
3.4.7.3. The electric field method.....	23
3.4.8. The image quality tests	24
Chapter 4 Results and Discussions.....	25
4.1. Modification of the terminal groups of poloxamer 407	25
4.2. The lower critical sol-gel temperature of poloxamer hydrogel	26
4.3. The mechanism properties of poloxamer hydrogel	27
4.4. Identification of titanium dioxide nanoparticles.....	28
4.5. Absorption and transparency of poloxamer hydrogel.....	29
4.6. Refractive index of poloxamer/titanium dioxide nanoparticles hybrids	30
4.7. Reconstruct the gradient refractive index structure using different methods..	32
4.8. Measuring the focal length based on PDMS capsule	36
4.9. The image quality tests	38
Chapter 5 Conclusion	39
Chapter 6 References	41

List of Figures

Figure 1. The human eye structure. ³⁸	44
Figure 2. (A)The normal, clear crystalline lens (B) cataract. ³⁹	44
Figure 3. The IOL surgery processes: (A) remove the pathological crystalline lens (B) the IOL inserted to the capsule (C) IOL final position. ⁴⁰	45
Figure 4. The different wound size according to the transplantation material (A) PMMA (B) soft artificial crystalline lens.	45
Figure 5. The gradient structure in the human crystalline lens. ⁴¹	46
Figure 6. The four steps of the Phaco—Ersatz theory (A) Cataract undergoes emulsification extraction (B) Capsule-zonule-ciliary body framework is maintained (C) Refilling with an ersatz material (D) Ersatz lens designed to preserve accommodation. ⁵	46
Figure 7. The reversible disulfide copolymer hydrogel system. ¹⁴	47
Figure 8. Strategy for spherical aberration correction in a convex lens. ³⁰	47
Figure 9. Steps to fabricate a polymer GRIN lens. ³⁰	48
Figure 10. Circular electrophoresis equipment and its working schema. ³¹	48
Figure 11. Modification of the terminal groups of poloxamer 407.	49
Figure 12. The sol-gel transition phenomenon (A) solution state (B) gelation state.....	49
Figure 13. Sol–gel transition and UV-induced photo-cross-linking of diacrylated poloxamer polymer.	50
Figure 14. The PDMS capsule filled with poloxamer hydrogel in the (A) stretch (B) unstretch state. (The diameter of the dime is 1.8 cm).....	51
Figure 15. The one-dimensional electric field method using in the experiment	52
Figure 16. Circular electrophoresis working schema (A) side view (B) top view.	52
Figure 17. The circular electron in the (A) profile (B) Lateral view (C) Top view (D)	

Experiment instrument.	53
Figure 18. The ¹ H-NMR spectrometries of (A) poloxamer 407 and (B) poloxamer 407A.	54
Figure 19. FTIR spectra of (A) poloxamer 407 and (B) poloxamer 407A.....	55
Figure 20. The lower critical sol-gel temperature of (A) poloxamer 407 and (B) poloxamer 407A.	55
Figure 21. UV–vis absorption of poloxamer hydrogel samples.....	56
Figure 22. The UV-vis transmittance of Human crystalline lens in different ages ⁹ and poloxamer hydrogel samples.	56
Figure 23. The Young’s modulus of the different ratio of poloxamer 407A/407 and concentration of initiator after irradiation for 60s.	57
Figure 24. The Young’s modulus of the different ratio of poloxamer 407A/407 and concentration of initiator after irradiation for 30s.	57
Figure 25. XRD patterns of titanium dioxide nano particles (lines:rutile phase JCPDS no. 89-4920).	58
Figure 26. The particle diameter distribution of titanium dioxide nanoparticles.	58
Figure 27. The refractive index of the different ratio of poloxamer 407 and 407A.	59
Figure 28. The refractive index of poloxamer hydrogel containing different concentration of titanium dioxide nanoparticles.	59
Figure 29. The lensmaker’s equation model.....	60
Figure 30. The stretch and unstretch focal length changes according to the different concentration of titanium dioxide nanoparticles.	60
Figure 31. (A) The distance of the lines through poloxamer hydrogel are equal before interface moving method (B) The distance of the lines through poloxamer hydrogel are decreasing after the interface moving method.....	61

Figure 32. Poloxamer hydrogel bulk moving phenomenon in the centrifuge method... 62

Figure 33. The moving rate with the different methods..... 62

Figure 34. The change of image quality according to the different times of electron field
at 5V/cm. 63

Figure 35. The change of image quality according to the different times of electron field
at 10V/cm. 64



List of Tables

Table 1. Physical properties material of the human lens contents and hypothetical values of an ideal ersatz ⁵	65
Table 2. Physicochemical characteristics of Pluronic [®] block copolymers ⁴²	66
Table 3. The concentration of poloxamer hydrogel in the sol-gel experiment.....	66
Table 4. The concentration of poloxamer hydrogel in the Mechanical properties test...	67
Table 5. Composition of the prepared poloxamer hydrogel containing titanium dioxide nanoparticles	67



Chapter 1 Introduction

Human crystalline lens is a plate like transparent lens, which contains about 65% water and 35% organic materials. Crystalline lens can change the shape by tighten or relax the ciliary muscle, so the objects in the different distance can be look clearly on the retina. (Figure 1)

The crystalline lens would loss its penetrability when increases of ages or exposes to external factors like UV-light. This chronic disease is called the cataract. The cataract will be a serious risk of blindness if there is no further treatment. (Figure 2)

According to statistics of the Department of Health, Executive Yuan, R.O.C.(Taiwan), cataract is the 2nd chronic disease in the aged person, about 42.53%, just lower than high blood pressure disease.¹

Artificial crystalline lens transplantation is the most common surgical treatment of cataract in recent years. (Figure 3) Traditional artificial crystalline lens is made from Poly (methyl methacrylate), also called PMMA. PMMA has good light transmittance, but in the room temperature, PMMA is a rigid polymer, therefore we need a larger wound in the process of artificial crystalline lens implantation, about 7-8 mm. (Figure 4)

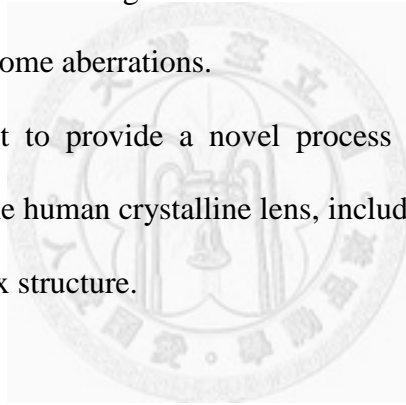
In recent years, the soft material for artificial crystalline lens was invented, so that the wound could be decreased down to 3-4mm, but still need a wound to put the artificial crystalline lens in. Current artificial crystalline lens is single-focus or multi-focuses, which can not provide the focusing function like the human crystalline lens. The mainly reason is the material we put into is too rigid, so the patients can not use the healthy ciliary muscles to change the focus. For this reason, an additional correction must be wearing.

Treatment method is still moving toward a smaller wound. If we can remove the

necrosis crystalline lens and save the crystalline lens capsule, then the injectable materials can be injected into the capsule by needles and forming the origin structure. Thus, the wound will be able to diminish than 1mm, and after injected into the crystalline lens, the shape of capsule is as same as the original human crystalline lens. This way can prevent some diseases due to the different shapes of the crystalline lens.

From the anatomy of human crystalline lens, we know that the crystalline lens is not made from homogenous materials. The crystalline lens can be roughly divided into two parts: The lens core group and the external organizations zone (Figure 5). The refractive index would variation from the core zone to the external zone according to the different density of proteins. This gradient refractive index structure can help the crystalline lens preventing some aberrations.

In this study we want to provide a novel process by the injection method to simulate the properties of the human crystalline lens, include the basic optical properties and gradient refractive index structure.



Chapter 2 Paper review

2.1. Injectable materials

In 1964 Kessle et al. team group² first using the liquid silicone materials to inject into the crystalline lens capsule of rabbits, and got a flexible crystalline lens. This new development of artificial lens has opened a new chapter – injected crystalline lens.

Injected crystalline lens implantation is a new technique that the researchers were researching on. This method can retain the completeness of the ciliary muscle, ciliary zonule and crystalline lens capsule, and injected the materials we development to replace the pathological changes of the crystalline lens.³ When the material was form a gelation state, the patients can change the crystalline lens curvature by using the origin ciliary muscle, just like human crystalline lens function.

There are some properties we should conform to near the real human crystalline lens:⁴

- (1) It should be injected into the crystalline lens capsule easily, and the materials do not leak from the capsule in the case if have external pressure.
- (2) The materials will not lead to inflammatory reaction, and have good biocompatibility.
- (3) The materials should have good optical properties. The degree of light penetration should reach 96% or more, the refractive index is about 1.41, and has the ability to filter UV-light.
- (4) The materials' density should a little bigger than the body fluid, and wouldn't swell in the water solution.
- (5) The materials can inject in the liquid solution, and use the physical or chemical reactions in the rapid cross-linked into an elastic gel state.

The detail properties is show in Table 1

Phaco—Ersatz theory⁵ thinks a success-injected crystalline lens should follow the four steps(Figure 6):

1. Cataract undergoes emulsification extraction
2. Capsule-zonule-ciliary body framework is maintained
3. Refilling with an ersatz material
4. Ersatz lens designed to preserve accommodation

2.1.1. Silicon gelation

In the early scientific or technical literature, most researcher groups appear to use poly (dimethyl siloxane), or called the PDMS as the material. The PDMS has the refractive index about 1.40 and density about 0.98g/cm³. By copolymerizing PDMS with other polymers, the refractive index of the materials can be increased and at the same time the specific gravity increases well over 1g/cm³. Such materials are used in high refractive index foldable crystalline lens.

Kessler et al. team group² uses the following materials as the ersatz material to simulate the human crystalline lens: hyaluronic acid, methylcellulose, silicone fluids (oils), epoxy gels, polyurethane gels, thixotropic compounds and silicone elastomers.

Agarwal et al. and Parel et al. team groups^{5, 6} use the silicon rubbers as the main material. This material is polymerization from the monomer which containing the silicon and other organics. The silicon rubber used in the medicine at middle of 20th, because this polymer is very stable in human body. The silicon rubber is a hydrophobic material, so the affinity between human body and material is very poor. The solidification time is about 12h, so the silicon material might be leaked out from the crystalline lens, forming some eye pathological changes. Eventually, a silicon material

was chosen as the most promising.

Sverker Norrby et al. team group⁷ uses a ter-copolymer as the main material, and combine the other materials as the cross-linker to form a cross-linked network structure. But there is no further statement about the materials.

2.1.2. Hydrogel

Hydrogel is another candidate for a crystalline lens material. The hydrogel does not like silicones, the hydrogel contains water, and they are still some questions about this material. The higher refractive index requires higher concentration of polymers, but too much polymers will make the hydrogel too viscous to inject or too hard to deformation. Therefore, polymers with high refractive index must be looked for. Hydrogel is intuitively attractive, as the hydrogel is felted to be closer to human crystalline lens. In fact, the human crystalline lens is a technically hydrogel building by different structures of proteins.

Hettlich et al. team group⁸ used the acrylate or methacrylate solution as the main materials. Using the UV irradiation, which wave length is about 400-500 nm, can cross-link the materials very quickly in the lens capsule, preventing the leakage of injected materials. But the materials in this experimental is too hard, and the refractive index is also too high (~1.51).

Groot et al. team group⁹ used the different molecular weight poly (ethyleneglycol) diacrylate and different percentage acrylate modified co-polymer of vinyl alcohol and N-vinyl pyrrolidone as the main material. The photo-initiator is the copolymer of (4-vinyl-2, 6-dimethylbenzoyl)-diphenyl phosphine oxide (4 mol %) and dimethyl acrylamide (96 mol %). The absorbed of this photo-initiator is in the blue light region, so the light damage on retinal can be reduced. The poly (ethyleneglycol)diacrylate has

high reactivity and high transparency, but the low viscosity will cause the leakage of materials. The co-polymer of vinyl alcohol and N-vinyl pyrrolidone is to increase the viscosity and the refractive index of the materials. When the co-polymers adjust to 50wt%, the refractive index is about 1.42. With the different percent acrylate modified group, the mechanical properties can be adjusted, too.

2.1.2.1. Pluronic tri-block-co-polymers¹⁰⁻¹²

Pluronic tri-block-co-polymer (also called “poloxamer”) is making up by polyethylene oxide (PEO) and polypropylene oxide (PPO). The PEO chain is a hydrophilic molecular, and the PPO chain is a hydrophobic molecular. This structure made poloxamer to be an amphiphilic copolymer. With different ratio of PEO and PPO chain length, let poloxamer has different characteristics, as show in Table 2.

Amphiphilic copolymer has self-assembling ability in the solution phase. The self-assembling structure will change from micelle to the hexagonal, and to the lamellar with different concentration or the different temperature.

Poloxamer is a PEO-PPO-PEO amphiphilic copolymer. When the concentration in the solution is higher than the critical micelle concentration (CMC), the solution will change from solution state to gelation state, or called the sol-gel transition. The sol-gel transition temperature is also called the lower critical sol-gel temperature (LCST). (Figure 12)

Ji Won, K. et al. team group¹¹ used poloxamer hydrogel as an injectable crystalline lens material, and to induce irreversible poloxamer hydrogel by UV irradiation. A mixture comprising 25% poloxamer and 0.01% photo initiator produced a poloxamer hydrogel that still have good transparency in the rabbits crystalline lens capsule for up to 6 months. But the refractive index of poloxamer hydrogel was 1.36,

and may be too low to be used for crystalline lens refilling.(Figure 13)

2.1.3. Polyurethane

Polyurethane is a polymer consisting of a chain of organic units joined by urethane links. Polyurethane polymers are polymerization by reacted a monomer which has at least two isocyanate functional groups with another monomer has at least two hydroxyl groups.

With the different types of isocyanate and hydroxyl monomers, polyurethane will has the different properties. Polyurethane has good mechanical strength, resistance to bending of elastic material, especially its biocompatibility, excellent chemical and physical stability.

Groot et al. team group¹³ used the different type of polyalcohols (PVA, PAA, PHP and EVA) and the different length diisocyanate (1, 4-butane-diisocyanate and 1, 12-dodecyldiisocyanate) as the cross-linker. The EVA co-polymer has good transparency, but the Young's modulus is too large (~1MPa). In the polyurethane system, it has the rod and coil chain. In aqueous solution is prone to phase separation, resulting in the polymer surface scattering phenomena, and the material of the light transmission rate. The experiment chooses the BDI-BDO-BDI as the block cross-linker, which can lower the reactivity and prevent the phase separation, obtaining a product of uniform and transparent material.

2.1.4. Disulfide gelation

Aliyar et al. team group¹⁴ used the acrylamide and N, N'-bis (acryloyl) cystamine to make the co-polymer. N, N'-bis (acryloyl) cystamine has S-S bond, which can be

broken by the dithiothreitol (dithiothreitol can break the S-S bonding to form of thiol group). The materials will change from gelation state to solution state. Injecting the solution state polymers with the 3,3'-dithiodipropionic acid in to the lens capsule. The 3,3'-dithiodipropionic acid can regenerate the S-S bond from the thiol group, so the material is change from solution state to gelation state. This material has the similar Young's modulus with human crystalline lens. But the refractive index of this material is too low. (Figure 7)

2.2. The high refractive index materials

With the development of practical optics, the optical properties of the material itself seem more important. The high refractive index materials in optical applications have their special value. When we use in the production of optical lenses, the lens thickness can be lower down according to the high refractive index material, so the optical components with high refractive index material can reduce the space, making a smaller, lighter optical components.¹⁵

There are several methods to increase the refractive index, in the organic or inorganic ways:

1. Combining the inorganic salts with the hydrogel; like PbS.¹⁶
2. Combining the polymer that has highly conjugated or aromatic-type with the hydrogel; like sulfur-containing aromatic methacrylates.^{17, 18}
3. Combining the metal oxide with the hydrogel; like titanium dioxide.¹⁹

2.2.1 Titanium dioxide^{20, 21}

Titanium dioxide has been studied widely according to its applications. In recent

years, nano-size titanium dioxide is well known as a semiconductor with photo catalytic activities

Titanium dioxide has very high refractive index, about 2.6-2.7, and titanium dioxide can be produced in the nano size to prevent the light scattering phenomenon.

Production of titanium dioxide nanoparticles can be divided into two reactants: the inorganic salt of titanium or the alkoxide of titanium.

Alkoxide of titanium is high purity and simple reaction, and most academics are using it as the starting reactant to produce titanium dioxide such as titanium butoxide $(\text{Ti}(\text{OBu})_4)^{22}$, or titanium ethoxide $(\text{Ti}(\text{OEt})_4)^{23}$. Because the hydrolysis of alkoxide titanium and water was too fast, so we need to react in the organic solution without water to prevent the larger particles produce. It is not useful in the water reaction system.

The inorganic salt is cheaper than the alkoxide of titanium. In the production process of titanium dioxide nanoparticles, first the inorganic salt of titanium can be reacted into titanium hydroxide, and use the acid solution to peptization the titanium hydroxide to get the titanium dioxide nanoparticles. All the reactions can be reacting in the water solution. It is more convenient for practical. The use of inorganic precursors rather than organic precursors not only reduces the cost of synthesis but also avoids the use of organic solvents that could cause pollution.

Natarajan Sasirekha et al. team group²⁴ used titanium tetrachloride as a precursor and reacted with an aqueous solution of ammonia solution to form titanium hydroxide, and hydrogen peroxide was then added to form peroxotitanic acid. The materials were characterized by XRD, FTIR, and TEM. The primary titanium dioxide particles were rhombus with the major 10nm and minor 4nm in anatase structure. The sol was excellent in dispersibility and was stable in neutral and even slight basic conditions with

out causing agglomeration.

2.3. Gradient refractive index (GRIN) structure

Traditional optical material is a homogeneous material so the refractive index for the material is a constant. In recent years, nanoparticles in optical applications have been developed such as modification on the refractive index of organic optical material.²⁵ A light is refracted because there is a different refractive index between the lens material and the air at the lens surface, the increasing refractive index of organic materials can cause stronger refracted effect.

This unique property in material refractive index improvement provides an opportunity to produce gradient refractive index (GRIN) structure in optical lens system. Gradient refractive index (GRIN) means the optical materials have a variation or gradient refractive index inside. GRIN lens can continually redirect the light beam to the focal point without the need of tightly-control the surface curvature. It can also ameliorate the Spherical aberration because of the GRIN structure. The curvature of the lens and the refractive index gradient in the material both can affect the focal length (Figure 8).

Current GRIN lens manufacturing methods are available only for glass material.²⁵ In recent years, researchers are invented numerous methods to make a GRIN lens using in the organic polymers. Different economic and effective methods have been explored, such as vapor phase transfer²⁶, swollen-gel polymerization²⁷ and organic-inorganic composite materials²⁸. Controlling the concentration of nanoparticles or the polymers in the organic material can adjust the refractive index. The nano-size particles play an important role to prevent the light scattering, particularly in the visible wave length (400-800 nm). A traditional lens design requires an aspheric surface to prevent spherical

aberration that decreases the optical quality.

Human crystalline lens is a radial gradient lens, where the refractive index decreases from the center to the edge. This distribution of radial gradients can add focusing power and lower the spherical aberrations. Recently, the highly refractive index nanoparticles-polymer composite materials have been developed. However, the fabrication of organic within gradient refractive index is still a challenge.

Franciscus G.H. et al. team group²⁹ use the MMA monomer and PTFPMA polymer as the materials. The refractive index of MMA is higher than PTFPMA; the density of MMA is lower than PTFPMA. When the homogeneous mixtures were in a centrifugal field, the heavier MMA was going toward out side of the tube to make the refractive index higher. Homogeneous mixtures were rotated at 20,000 rpm for 24 hours, and the refractive index would decrease from center to the edge of the tube, forming the gradient refractive index structure.

J.S. Shirk et al. team group³⁰ used the polycarbonate (PC) and polymethyl methacrylate (PMMA) coextruded from the two single-screw extruders. By adjusting the melt pump speed the ratio of PC to PMMA can be varied. Combining the different ratio of PC and PMMA films layer by layer, the refractive index can increase from center (1.58) to edge (1.49) continuously. Figure 9 shows the layer-by-layer method can create a lens with gradient refractive index, but those materials are too hard to use in the crystalline lens.

Weisong Wang et al. team group³¹ used the silica nanoparticles and polyacrylamide hydrogel as the main material. Figure 10 shows that silica nanoparticles were moving toward the opposite charged electrode and distributed according to the electrical field. The electrical field phenomena have also been used with a circular electrode. The experiment data were examined by film measurement system and XPS. It has been

proven that electrical field in hydrogel film that presents the radial gradient refractive index profiles could control the distribution of nanoparticles.



Chapter 3 Experiment

3.1. Experiment materials

#	Material	Purity	Provider
1	Pluronic F-127 (Poloxamer 407)	-	Sigma
2	Acryloyl chloride	96%	Alfa Aesar
3	Triethylamine	99%	Acros
4	Tetrahydrofuran	-	Mallinckrodt
5	n-Hexane	-	Mallinckrodt
6	Titanium (IV) chloride	99.9%	Acros
7	Sodium hydroxide	-	Fisher scientific
8	Hydrochloric acid	36%	Fisher scientific
9	2-Hydroxy-4'-(2-hydroxy-ethoxy)-2-methylpropiophenone	98%	Aldrich

3.2. Experiment Instruments

1. Fourier Transform Infrared Spectroscopy

The Fourier Transform Infrared (FTIR) absorption spectra were recorded between 4000 and 400 cm^{-1} to identify the terminal function groups in poloxamer.

2. Nuclear Magnetic Resonance

The terminal function groups in poloxamer polymer were examined by using the NMR (BRUKER, AVANCE 400) in the D-chloroform solution.

3. Abbe Refractometer

Measure all poloxamer hydrogel which containing different ratio alkene groups or titanium dioxide nanoparticles using the Abbe Refractometer (Atago&Tokyo, E1-243) at the wavelength 589.1 nm.

4. Tension

The mechanism properties of poloxamer hydrogel samples were examined by using the Tension in the rate 5mm/min and stop when the strain is 40%. The Young's modulus was calculated from slope of the stress-strain curve.

5. Lithography Steppers

All poloxamer hydrogel which containing alkene group are cross-linked by using the Lithography Steppers (Jiann-Haur, JH-1000C) in the $10\text{mW}/\text{cm}^2$ at the wavelength UV-light region.

6. UV-vis Spectrometer

The absorptions of all poloxamer hydrogel were performed using the UV-vis spectrometer (Thermo Spectronic, HeλIOSγ). The concentration of all samples were the original concentration and measure in a 1 cm path length cuvette.

7. X-ray Diffraction

X-ray diffraction study (Philips, X'PERT), using $\text{CuK}\alpha$ radiation at 40KV and

40mA, was conducted to examine the crystalline phase of titanium dioxide particles

8. Particle Size Analyzer

The size of the titanium dioxide particles distribution was investigated using a Malvern (Nano-ZS).

9. Auto Lensmeter

The focal length of PDMS capsule lens containing different refractive index poloxamer hydrogel was measured by auto lensmeter in the unit Diopter.



3.4. Experiment Methods

3.4.1. Modification of the terminal groups of poloxamer 407³²

15g of poloxamer 407 was dissolved in 80 ml of tetrahydrofuran (THF) and blended until being completely dissolved. When the poloxamer 407 was dissolved, 0.67 ml of triethylamine and 0.39 ml of acryloyl chloride were added and the reaction takes place for 24 hrs at 60°C. After the reaction, the solution was under gravitational filtration to remove white salt precipitation to obtain a transparent end-modified polymer THF solution. And then the end-modified polymer THF solution was slowly added into 240 ml of n-hexane. The solution was blended by a stirrer to separate out the end-modified polymer. Then, vacuum filtration was used to remove n-hexane so that white precipitate of the end-modified polymer was obtained. Finally, the white precipitate of the end-modified polymer was dried by an oven at 50°C for 24 hrs and thus puffy white powders of the end-modified poloxamer polymer (poloxamer 407A) were obtained. The reaction step was show in Figure 11.

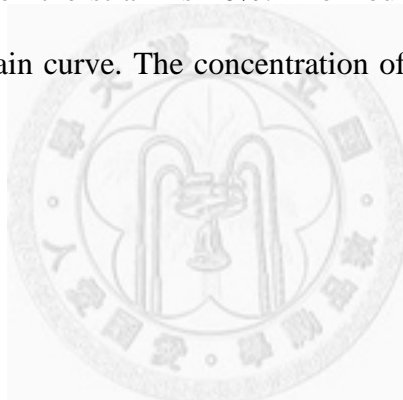
3.4.2. The lower critical sol-gel temperature of poloxamer hydrogel

Poloxamer 407 or poloxamer 407A was dissolved in deionized water to obtain the polymer solution which containing different concentration of poloxamer 407 or poloxamer 407A in 20ml vials, as show in Table 3. The vials were in the water bath which increasing the temperature at the rate $1^{\circ}\text{C}/\text{min}$ from room temperature to 50°C , the lower critical sol-gel temperature of poloxamer 407 and poloxamer 407A was determined when the samples did not drop or slip from inverted vials, as show in Figure 12.



3.4.3. The mechanism property of poloxamer hydrogel

The different ratio of poloxamer 407 and poloxamer 407A was dissolved in 4.1 ml deionized water. And then the different concentration of photoinitiator (2-hydroxy-4'-(2-hydroxy-ethoxy)-2-methylpropiophenone) was added to the mixed polymer solution and injected 2ml polymer solution into a 1cm x 1cm x 2.5 cm transparent containers. The UV irradiation was used to initiate the reaction of cross-linking with different times at the light intensity 10 mW/cm^2 . The container was removed to obtain the 1cm x 1cm x 2cm poloxamer hydrogel sample. The mechanism properties of poloxamer hydrogel samples were examined by using the Tension in the rate 5mm/min and stop when the strain is 40%. The Young's modulus was calculated from slope of the stress-strain curve. The concentration of materials in the experiment was show in Table 4.



3.4.4. Preparing the titanium dioxide nanoparticles

20 ml of titanium tetrachloride was placed in an ice bath and 50 ml of ice was added to obtain a light sticky liquid. Under the ice bath, 10M sodium hydroxide solution was added slowly into the above solution until the pH reach 7 and a large amount of white solids were separated out. Then using the vacuum filtration to filtrate the white solids. After the solution was removed, white clay titanium hydroxide ($\text{Ti}(\text{OH})_4$) cake was obtained. The cake of titanium hydroxide was mixed with 500 ml of dH_2O again and blended until being completely mixed. Repeat the washing and vacuum filtration steps at least three times, in order to remove the chloride ions completely. titanium hydroxide cake was placed in a centrifuge at 9000rpm for 20 minutes to remove the remnant water. In order to get the titanium dioxide nanoparticles solution, 0.3 ml of 36% hydrochloride is added into 1g of titanium hydroxide cake and blended violently for 30 minutes to obtain a transparent titanium oxide nanoparticles solution. The solution dry in the 60°C oven for 24 hrs in order to remove the solvent, and the white titanium dioxide powders was getted. XRD and Particle size analyzer were used to inspect the crystal phase and crystal size.

3.4.5. Refractive index of poloxamer/titanium dioxide nanoparticles hybrids

0.3 ml of 37% hydrochloride was added into 1g of titanium hydroxide cake and blended violently for 30 minutes to obtain a transparent titanium oxide nanoparticles solution. Different amount of deionized water was added separately and blended until becoming uniform. The poloxmer was added and blended under the ice bath until dissolved to obtain a polymer solution containing 2.5/5/7.5/10 wt% of titanium oxide, the detail concentration is show in Table 5. Using the Abby refractometer to measure the refractive index at the wave length 589.1 nm.



3.4.6. Measuring the focal length based on PDMS capsule

Polydimethylsiloxane (PDMS) prepolymer (A) and curing agent (B) were mixed together in the weight ratio 10:1, and using a vacuum pump to remove air bubbles generated from mixing. The PDMS solution was poured slowly into the mold until the mold is full up, and then combined the top and bottom molds carefully to prevent bubble generation. The curvature of the mold was $0.06r^2$ (in mm)for up and down, and the thickness of the PDMS membrane was $810\ \mu\text{m}$. Placing the mold in 60°C oven for 12 hours, and strip away the mold after solidify to obtain the PDMS membranes. Bonding two pieces of PDMS membranes together and get a hollow imitation of the crystalline lens capsule. Poloxamer hydrogel solution containing different concentration of titanium dioxide nanoparticles injected with an 18# needle, and then increases the temperature to occur sol-gel transition to prevent the leakage. The UV irradiation was used to irradiate the reaction of cross-linking at the intensity $10\ \text{mW}/\text{cm}^2$. Place the PDMS capsule in 1% agar gelation to simulate the environment of human crystalline lens, and using the clamps to imitate the stretch and unstretch state to measure the focal length changes, the experiment samples were show in Figure 14.

3.4.7. Reconstruct the 1-dimension gradient refractive index structure

2 ml of poloxamer solution was injected into a 1cm x 1cm x 5cm transparent container. Then increasing the temperature to 35°C, poloxamer solution was changed to the gelation state by sol-gel transition. 1 ml poloxamer solution containing 10 wt% titanium dioxide nanoparticles was added above the gelatinoids poloxamer hydrogel at the 35°C. Using a paper with equal width lines as the background and through this method to observe the change of the lines to determine moving distance, as show in Figure 31.

3.4.7.1. The Fick's law diffusion method

The container deposed in the horizontal state to prevent the gravity force movement, and observe the change every 8 hrs, till 72 hrs at the 30°C.

3.4.7.2. The centrifuged method

The container was deposed in the centrifuge and rotated in different rpm and times, and observed the change every 5min, till the moving distance was larger than 0.5 cm.

3.4.7.3. The electric field method

The container deposed in the horizontal state to prevent the gravity force. The positive plate electrode was inserted in poloxamer hydrogel which containing 10 wt% titanium dioxide nanoparticles side and the negative plate electrode was inserted at poloxamer hydrogel without titanium dioxide nanoparticles. Accessing the different electric field from 5V/cm and 10V/cm to move the titanium dioxide nanoparticles, and observed the change every 5min, till the moving distance was larger than 0.5 cm. The experiment instrument was show in Figure 15.

3.4.8. The image quality tests

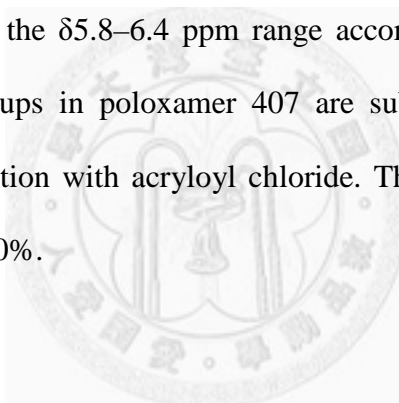
Polydimethylsiloxane (PDMS) prepolymer (A) and curing agent (B) were mixed together in the weight ratio 10:1. Using a vacuum pump to remove air bubbles generated from mixing. The PDMS solution was poured slowly into the mold until the mold is full up, and then combined the top and bottom molds carefully to prevent bubble generation. The mold size was same which used in experiment 3.4.6. Place the mold in 60°C oven for 12 hours, and strip away the mold after solidify to obtain the PDMS membranes. Bonding two pieces of PDMS membranes together and we can get a hollow imitation of the crystalline lens capsule. Poloxamer solution will be injected with 18# needles, and then increase the temperature to 35 °C to occur sol-gel transition to prevent the leakage. Poloxamer solution containing 10% titanium dioxide nanoparticles was injected into the middle of the crystalline lens capsule sample to form the high refractive index core. The crystalline lens capsule sample was placed between two circular electrodes tightly to prevent non-contact phenomenon. Applying the voltage between the outside and central electrode, the titanium dioxide nanoparticles will move toward the oppositely charged electrode to create the gradient refractive index structure, as show in Figure 16. Using the grid picture as the background to observe the image change in the different voltage and times. The circular electron instrument using in the experiment was show in Figure 17.

Chapter 4 Results and Discussions

4.1. Modification of the terminal groups of poloxamer 407

Poloxamer 407A is synthesized from the reaction of poloxamer 407 by using acryloyl chloride. Figure 19 shows poloxamer 407A has a new absorption band at 1723 cm^{-1} , appoint to the C=O stretching vibration because of acrylation, which is lacking in poloxamer 407 itself. Poloxamer 407 and poloxamer 407A both show an absorption band at 1110.7 cm^{-1} , assign to the C-O-C stretching vibration.

The formation of poloxamer 407A is confirmed through $^1\text{H-NMR}$ spectrometry. Figure 18 shows the $^1\text{H-NMR}$ spectrum has three peaks in the vinyl groups of poloxamer 407A appear in the $\delta 5.8\text{--}6.4$ ppm range according to the acrylate groups. The terminal hydroxyl groups in poloxamer 407 are subsequently converted to the acrylate groups by the reaction with acryloyl chloride. The substitution degree of the poloxamer 407 was about 70%.



4.2. The lower critical sol-gel temperature of poloxamer hydrogel

Thermo-reversible transition is a unique characteristic of poloxamer, which depends on the concentration and the ratio of PEO in poloxamer. To observe the effect of sol-gel transition of poloxamer 407, the lower critical sol-gel temperature tests of poloxamer 407 and poloxamer 407A are examined.

Figure 20 shows the lower critical sol-gel temperature decrease when increase the concentration of poloxamer 407 or 407A, and poloxamer 407A shows similar sol-gel behavior with poloxamer 407. When the concentration is lower than 16wt%, poloxamer 407A can not form a gelation state because the original terminal hydrophilic hydroxyl groups of poloxamer are reacted into the hydrophobic acrylate groups. The sol-gel transition phenomenon of poloxamer is known as a self-assembling mechanism, so the effect of terminal group modification on the sol-gel of poloxamer 407 is significant. The different lower critical sol-gel temperature between poloxamer 407 and 407A is clearly when the concentration is under 20wt% according to the properties of the terminal groups. But when the concentration is higher than 22wt%, the difference is nearly disappearing, because the increasing concentration of poloxamer can lower the terminal acrylate effect. Temperature of human body is about 37°C, so we choose the 18wt% as the experiment concentration. The sol-gel temperature for 18wt% poloxamer solution is about 25-28°C, just little higher than the room temperature and lower than Human body. We do not choose the 16 wt% to prevent the critical situation appears in the experiments.

4.3. The mechanism properties of poloxamer hydrogel

To determine the Young's modulus of poloxamer hydrogel samples, tension tests are performed under a constant compression rate at 5mm/min. The Young's modulus would determine from slope of the strain-stress curves.

Figure 23 and Figure 24 show the Young's modulus of poloxamer hydrogel samples change significant when increase the ratio of poloxamer 407 or decrease UV irradiation times. Poloxamer hydrogel which make from pure poloxamer 407A and irradiate for 60s shows the highest Young's modulus, about 250kPa. The other side, poloxamer hydrogel which make from 10 wt% poloxamer 407A, 8 wt% poloxamer 407 and irradiation for 30s shows the lowest Young's modulus, about 18kPa. We also decrease the concentration of photo initiator from 0.05 wt% to 0.025 wt%, but the experiment data show there is no distinguishability between each other. When we want to increase the ratio of poloxamer 407 or decrease UV initiation times to let the Young's modulus fitted the human crystalline lens ($\sim 1.5\text{kPa}$)³³, the samples would be too soft so we even can not remove the hydrogel from the mold. Although the Young's modulus of poloxamer hydrogel may closer to the human crystalline lens, but if poloxamer hydrogel still has the mobility, it is bad for maintain the structure of crystalline lens or the gradient structure we want to make. Because the above views, we choose the hydrogel with 10 wt% poloxamer 407A, 8wt% poloxamer 407, 0.05wt% photo initiator and irradiation for 30s as the nearest one.

4.4. Identification of titanium dioxide nanoparticles

In order to increase the refractive index of poloxamer hydrogel, the titanium dioxide nanoparticles is introduced using the titanium chloride as titanium source. Titanium chloride through hydrolysis, adjust the pH, precipitate and acid-peptization processes, the titanium dioxide nanoparticles solution can be obtained. By drying the solution which contains titanium dioxide nanoparticles in 60°C oven for 24 hrs, the titanium dioxide nanoparticle is obtained. Comparison with the original weight, the solid ratio in the titanium hydroxide is about 20±1wt%. The reducing weight is from the water which contains in the titanium hydroxide and the by-products which in the acid-peptization process.

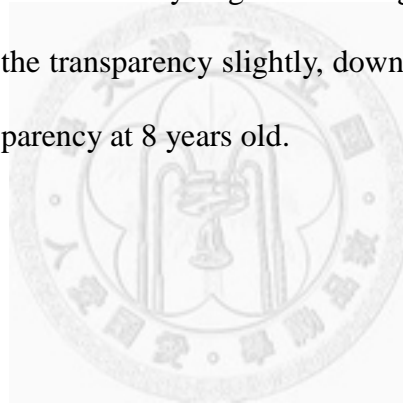
Figure 25 shows the XRD patterns of the titanium dioxide nanoparticles, which made from acid-peptization of the titanium hydroxide. We can find out all the XRD peaks correspond to rutile phase ($2\theta = 27.495, 36.154, \text{ and } 54.442$) according to PDF 89-4920. The data show that rutile nanocrystalline was formed. And the experiment data shows the same crystal phase when the pH in the acid-peptization step is lower.³⁴ Figure 26 shows the primary titanium dioxide nanoparticles in the particle diameter distribution has a nano-size about 11 nm. The refractive index of rutile phase crystalline is about 2.6³⁵, so we think when adds the titanium dioxide nanoparticles into poloxamer hydrogel can help us to increase the refractive index of poloxamer hydrogel.

4.5. Absorption and transparency of poloxamer hydrogel

Poloxamer solution, Poloxamer gelation and poloxamer hydrogel containing 0wt% or 10wt% of titanium dioxide nanoparticle are prepared to measure the absorption and transparency.

Figure 21 shows all samples have no absorption in the visible region, 400 to 800 nm. Poloxamer hydrogel containing 10wt% of titanium dioxide nanoparticles filters out most of the UV light and a considerable part of the blue light, due to the titanium dioxide is a photocatalysis.

Figure 22 shows the pure poloxamer hydrogel has a very high transparency even at the 18 wt%, is about 95%. Poloxamer hydrogel containing 10wt% of titanium dioxide nanoparticles will decrease the transparency slightly, down to 90%, but still higher than human crystalline lens transparency at 8 years old.



4.6. Refractive index of poloxamer/titanium dioxide nanoparticles hybrids

The refractive index of poloxamer hydrogel containing different concentration of titanium dioxide nanoparticles is measured by Abbey refractometer.

Figure 27 shows the different ratio of poloxamer 407 and poloxamer 407A hydrogel mixture has the almost same refractive index, about 1.355. The experiment data show the terminal groups of poloxamer 407A will not affect the refractive index obviously.

Figure 28 shows the refractive index of poloxamer hydrogel containing titanium dioxide nanoparticles increases when the concentration of titanium dioxide nanoparticles increases. The refractive index increases from pure poloxamer hydrogel, about 1.355, to poloxamer hydrogel containing 10wt% titanium dioxide nanoparticles, to 1.407.

The refractive index is an important property for the optics system and for the material. The refractive index for the mixture is also a function of the material's density, molar volume and mass. The refractive index for the mixed material can be calculated from the Lorentz-Lorenz equation:

$$n = \left(\frac{\sum_i x_i n_i^2 f_i}{\sum_i x_i f_i} \right)^{\frac{1}{2}} \quad (1)$$

$$f_i = \frac{\frac{m_i}{\rho_i}}{\sum_i \frac{m_i}{\rho_i}} \quad (2)$$

n_i = The refractive index for i material

f_i = The volume ratio for the i material

m_i = The mass for the i material

ρ_i = The density for the i material

According to the Lorentz-Lorenz equation, we can calculate the theoretical values to examine the experiment data are consisting or not. Figure 28 shows the experiment data can be fitted to the theoretical values, which are calculated from the Lorentz-Lorenz equation. The refractive index of Human crystalline lens is nearly 1.41~1.42, so we think poloxamer hydrogel containing 10wt% of titanium dioxide nanoparticles is practical.



4.7. Reconstruct the gradient refractive index structure using different methods

The pure poloxamer hydrogel or poloxamer hydrogel containing titanium dioxide nanoparticles are all transparency, so it is difficult to confirm the position of interface. We use a paper with equal width lines as the background so we can through this method to observe the change of the lines to determine the position of the interface.

Figure 31 shows the different line width between pure poloxamer hydrogel state and poloxamer hydrogel which has gradient refractive index structure. Pure poloxamer hydrogel shows the same line width because the refractive index in the pure poloxamer hydrogel is a constant. Poloxamer hydrogel which has gradient refractive index structure shows the line width is decreasing when closer to the high refractive index zone. The different line width change can help us to determine the length of interface going.

The Fick's law diffusion method

Fick's law diffusion is a time-dependent process, organized by random movement and causing the statistical distribution. The idea of diffusion is based on mass transfer, driven by the concentration difference. Unfortunately, the moving rate for this system is too slow. The interface spent three days but only moving about 3mm. According to Fick's law of diffusion:

$$l = 2\sqrt{Dt} \quad (3)$$

l = The moving length

D = The diffusion coefficient

t = Moving time

The diffusion coefficient for this system is about $8.68E-8$ cm²/s, which is intermediate between liquid and solid values since poloxamer hydrogel is gelation. The

moving rate is too slow so it is not a good method in the convenient and practical way.

The centrifuge method

A centrifuge is an equipment which puts objects in rotation around a fixed axis, and applies a centripetal force vertically to the axis. The centrifuge works using the sedimentation theory, where the centripetal acceleration makes heavier materials to separate out along the radial direction.

The density of the titanium dioxide is about 4.5 to 5 g/cm³, which is higher than poloxamer hydrogel, so the titanium dioxide nanoparticles will separate from the topside to the bottom side to form the gradient. Figure 32 shows in the centrifuge process, we find out the viscosity for poloxamer hydrogel is too high, therefore the whole poloxamer hydrogel containing titanium dioxide nanoparticles will move toward the bottom side in the bulk state. For this reason, we try to cross-link the bottom poloxamer hydrogel first to prevent the bulk-moving situation. Figure 33 shows the moving rate increase when centripetal acceleration increases from 1000 rpm to 5000 rpm. When the centripetal acceleration is higher than 5000 rpm, the centripetal force is too strong so the container will crack from the edge.

According to the centrifugal force equation:

$$F \propto r\omega^2 \quad (4)$$

F = Centrifugal force

r = Rotational radius

ω = Angular velocity

The radius we use in the experiment was about 8cm, but the crystalline lens radius is only about 0.4cm. We have to speed up the angular velocity to maintain the same centrifugal force to maintain the centrifuge effect. It is not convenient for gradient

refractive index forming and polymer hydrogel moving in the bulk state is still a problem. The centrifuge is an effective method to forming the gradient refractive index structure, but it is not suitable for the gradient refractive index forming in this experiment system.

The electric field method

An electric field is a property that describes the space that surrounds electrically charged particles. This electric field exerts a force on other electrically charged objects.

The isoelectric point (PI) of titanium dioxide is about pH 5-7. When the pH value is lower than the PI, the particles will carry the positive charge, otherwise will carry the negative charge³⁶. The pH value in the experiment is lower than the PI of titanium dioxide, so the nanoparticles will carry the positive charge. When we fixed the electric field between two electrodes, the titanium dioxide nanoparticles will move from the positive electrode side to the negative electrode side. Titanium dioxide nanoparticles were the only charged material in poloxamer hydrogel, so we can ignore the other materials affection.

Figure 33 shows the moving rate by the electric field method is higher than other two methods even in only 5V/cm. The only charged material in poloxamer hydrogel was the titanium dioxide nanoparticles, so we should not cross-link poloxamer hydrogel first to prevent the bulk poloxamer hydrogel moving which we found out in centrifuge method.

The electric field is defined as follow equation:

$$F = Eq \tag{5}$$

$F =$ Electric force

$E =$ Electric field

$q =$ Charge of the particles

When we double the electric field from 5V/cm to 10V/cm, the moving rate also increases from 1mm/6min to 1mm/3min. The higher electric field may speed up the moving rate of the titanium dioxide nanoparticles, but the higher voltage might provide too many energy to cause the temperature of poloxamer hydrogel increasing. The electric field can be designed in the different shapes according to the electrode structure, so it is possible to make the circular shape electric field to help us forming the gradient refractive index crystalline lens.



4.8. Measuring the focal length based on PDMS capsule

The focal length of the PDMS capsule is measured by the autolensmeter. All poloxamer hydrogel inject into the PDMS capsule successfully through #18 syringes. The PDMS capsules were fully refilled with poloxamer hydrogel, leaving nonnoticeable intracapsule space for further refilling. Poloxamer hydrogel did not leak from the capsule after refilling because when increase the temperature above the lower critical sol-gel temperature, poloxamer hydrogel change from solution state to gelation state according to the sol-gel transition phenomenon.

The PDMS capsule fill with poloxamer hydrogel is fixed in the 1wt% agar gel to simulate the environment of human crystalline lens.

The stretch and unstretch state is using clamps to clamp the PDMS membrane, so we can tighten the ropes that connected at the clamps to change the PDMS capsule curvature like human ciliary muscles.

Figure 30 shows the unstretch PDMS capsule power increase from 4.2D to 13.875D, and the stretch state increase from 3.33D to 11.35D when we increase the concentration of titanium dioxide nanoparticles in poloxamer hydrogel from 0wt% to 10wt%. The force we apply to the clamp nearly 200g, and the diameter of the PDMS capsule will change from 1.8cm to 2cm.

According to the lensmaker's equation⁶:

$$r_0 = \frac{(h^2 + r^2)}{2h} \quad (6)$$

$$\frac{1}{f} = \frac{2(n_2 - n_1)}{r_0} + \frac{(2h + d)(n_2 - n_1)^2}{r_0^2 n_2} \quad (7)$$

$$D \equiv \frac{100}{f} \quad (8)$$

- $f =$ Focal length
- $n_1 =$ The refractive index of environment material
- $n_2 =$ The refractive index of the crystalline lens material
- $h =$ The thickness of the PDMS capsule
- $d =$ The thickness of the PDMS membrane
- $r =$ The radius of the PDMS capsule
- $r_0 =$ The curvature of the PDMS capsule
- $D =$ Diopter

The curvature of the PDMS capsule can be calculated from equation 6, and the refractive index of poloxamer hydrogel was measured from experiment 4.6. We can calculate the diopter from equation 7 and 8 to compare with the experiment data.

The data which calculated from the lensmaker's equation are all conform to the experiment data, and show the same tendency of PDMS capsule power between stretch and unstretch state when the concentration of titanium dioxide in poloxamer hydrogel increased.

The change power of the PDMS capsule is about 16.57%, which is better than Human crystalline lens, about 8.37% ($20.8 \pm 5.3D$ to $22.7 \pm 2.4D$)³⁷.

4.9. The image quality tests

Spherical aberration is an optical effect observed in an optical instrument due to the increased refraction of light rays when they strike a lens. The focusing power of lens edge is stronger than the center, so the light can not focus in one point. According to this reason, it results in an imperfection of the produced image.

For the purpose of decreasing the aberration of lens, the gradient refractive index is introduced. The refractive index in the center is higher than the edge, so the focusing power in the center will be enhanced. The gradient refractive index usefulness is just like other lens, which can amend the path of light.

Figure 34 and Figure 35 show the image quality through the PDMS capsule that contains the gradient refractive index structure by electric field method. We inject the high refractive index poloxamer hydrogel containing 10wt% titanium dioxide nanoparticles in the center of the PDMS capsule. The focal point in the center is shorter than the edge due to the high refractive index, so the image in the center is blurred because there is an intercept between the low and high refractive index poloxamer hydrogel. By using the electric field in the different electric field strength and times, the image becomes clearer according to the gradient refractive index forming gradually. The refractive index of poloxamer hydrogel decrease from the center to edge, so the focal length will increase oppositely, so the focal point will focus on the same point to form the clearly image. The stronger the electric field, the less time would consume to get the same moving distance.

The image quality tests also prove again the electric field method can move the titanium dioxide nanoparticles in the circular form electron, according to the results in the reconstruct gradient refractive index structure experiment.

Chapter 5 Conclusion

In this article, a practical material for injected crystalline lens is investigated. We use poloxamer 407 that has the thermo-sensitive property as the main material. By acrylate the terminal groups from hydroxyl groups to acrylate groups, poloxamer hydrogel can be cross-linked by the UV irradiation. Using the different ratio of poloxamer 407A/407, UV irradiate times and concentration of photo initiator, we can adjust the Young's modulus of poloxamer hydrogel. In order to increase the refractive index to near the human crystalline lens, titanium dioxide nanoparticles was introduced into poloxamer hydrogel. The PDMS capsule is used as the bionic crystalline lens, and using the claps to simulate the focal length change under the stretch or unstretch state. Using the electric field method to reconstruct the gradient refractive index is also test in the experiment.

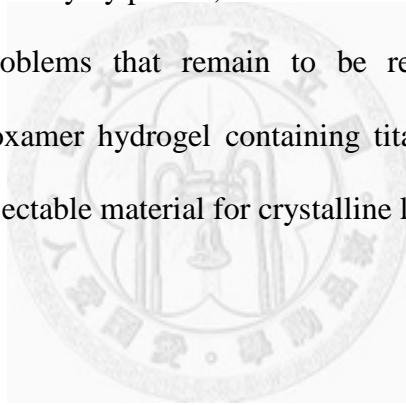
1. The lower critical sol-gel temperature of poloxamer 407A is higher than poloxamer 407 according to the terminal function groups. The different lower critical sol-gel temperature between 407A and 407 is significant when the concentration under 20wt%, but not significant above 22%.
2. Young's modulus of poloxamer hydrogel decrease from 230kPa to 18kPa when increase the ratio of poloxamer 407 and decrease UV irradiate times, but the concentration of photo initiate is not obviously.
3. The refractive index increase from 1.355 to 1.407 when introduce the titanium dioxide nanoparticles from 0wt% to 10wt% into poloxamer hydrogel, and the experiment data also can be fitted to the Lorentz-Lorenz equation theory value.
4. The diopter by using stretch or unstretch PDMS capsule shows the higher refractive index of poloxamer hydrogel will have larger diopter, and the different diopter change between stretch and unstretch state is also larger, too. All

experiment data are fitted by the lensmaker's equation values, which are calculated according to the curvature and refractive index of samples.

5. The gradient refractive index structure by using the electric field method also success and pragmatic even at 5V/cm, this method also prevents the bulk-moving phenomenon that appears in the centrifuge method. The image quality tests show the gradient refractive index structure can make the image clearly.

However, the stability of titanium dioxide nanoparticles is not test in the experiment, the refractive index of poloxamer hydrogel still a little lower than human crystalline lens (1.42), and the image quality of the crystalline lens that has gradient refractive index structure test only by photos, still needs some accurate valves.

Regardless of the problems that remain to be resolved, the results of the experiment data show poloxamer hydrogel containing titanium dioxide nanoparticles has the potential to be an injectable material for crystalline lens.



Chapter 6 References

1. Department of Health, Executive Yuan, R.O.C.(Taiwan)
2. Kessler, J., EXPERIMENTS IN REFILLING THE LENS. *Arch Ophthalmol* **1964**, 71, 412-7.
3. Reiner, J.; Speicher, L., Properties of injectable intraocular lenses. *Klin Monbl Augenheilkd* **1993**, 202, (1), 49-51.
4. Assia, E. I., Accommodative intraocular lens: a challenge for future development. *J CATARACT REFRACT SURG* **1997**, 23, (4), 458-60.
5. Parel, J.; Gelender, H.; Trefers, W.; Norton, E., Phaco-Ersatz: Cataract surgery designed to preserve accommodation. *Graefe's Archive for Clinical and Experimental Ophthalmology* **1986**, 224, (2), 165-173.
6. Agarwal, M.; Gunasekaran, R. A.; Coane, P.; Varahramyan, K., Polymer-based variable focal length microlens system. *Journal of Micromechanics and Microengineering* **2004**, 14, 1665-1673.
7. Norrby, S.; Koopmans, S.; Terwee, T., Artificial crystalline lens. *Ophthalmol Clin North Am* **2006**, 19, (1), 143-6, vii.
8. Hettlich, H. J.; Lucke, K.; Kreiner, C. F., Light-induced endocapsular polymerization of injectable lens refilling materials. *Ger J Ophthalmol* **1992**, 1, (5), 346-9.
9. de Groot, J. H.; van Beijma, F. J.; Haitjema, H. J.; Dillingham, K. A.; Hodd, K. A.; Koopmans, S. A.; Norrby, S., Injectable Intraocular Lens Materials Based upon Hydrogels. *Biomacromolecules* **2001**, 2, (3), 628-634.
10. Han, Y. K.; Kwon, J. W.; Kim, J. S.; Cho, C. S.; Wee, W. R.; Lee, J. H., In vitro and in vivo study of lens refilling with poloxamer hydrogel. *Br J Ophthalmol* **2003**, 87, (11), 1399-402.
11. Ji Won, K.; Young Keun, H.; Woo Jin, L.; Chong Su, C.; Seung Joon, P.; Dong Il, C.; Jin Hak, L.; Won Ryang, W., Biocompatibility of poloxamer hydrogel as an injectable intraocular lens: A pilot study. *Journal of cataract and refractive surgery* **2005**, 31, (3), 607-613.
12. Escobar-Chavez, J. J.; Lopez-Cervantes, M.; Naik, A.; Kalia, Y. N.; Quintanar-Guerrero, D.; Ganem-Quintanar, A., Applications of thermo-reversible pluronic F-127 gels in pharmaceutical formulations. *J Pharm Pharm Sci* **2006**, 9, (3), 339-58.
13. de Groot, J. H.; Spaans, C. J.; van Calck, R. V.; van Beijma, F. J.; Norrby, S.; Pennings, A. J., Hydrogels for an Accommodating Intraocular Lens. An Explorative Study. *Biomacromolecules* **2003**, 4, (3), 608-616.

14. Aliyar, H. A.; Hamilton, P. D.; Ravi, N., Refilling of ocular lens capsule with copolymeric hydrogel containing reversible disulfide. *Biomacromolecules* **2005**, 6, (1), 204-11.
15. Matsuda, T.; Funae, Y.; Yoshida, M.; Yamamoto, T.; Takaya, T., Optical material of high refractive index resin composed of sulfur-containing aromatic methacrylates. *Journal of Applied Polymer Science* **2000**, 76, (1), 50-54.
16. Kyprianidou-Leodidou, T.; Caseri, W.; Suter, U. W., Size Variation of PbS Particles in High-Refractive-Index Nanocomposites. *The Journal of Physical Chemistry* **1994**, 98, (36), 8992-8997.
17. Rogers, H. G.; Gaudiana, R. A.; Hollinsed, W. C.; Kalyanaraman, P. S.; Manello, J. S.; McGowan, C.; Minns, R. A.; Sahatjian, R., Highly amorphous, birefringent, para-linked aromatic polyamides. *Macromolecules* **1985**, 18, (6), 1058-1068.
18. 傅雅卿; 林唯芳, Synthesis and Physical Properties of High Refractive Index Epoxy Resins 國立台灣大學材料科學與工程學研究所碩士學位論文 **2001**.
19. Yoshida, M.; Lal, M.; Kumar, N.; Prasad, P., TiO₂ nano-particle-dispersed polyimide composite optical waveguide materials through reverse micelles. *Journal of Materials Science* **1997**, 32, (15), 4047-4051.
20. 周德瑜; 蔣孝澈, 四氯化鈦之控制水解研究 國立中央大學化學工程研究所碩士論文 **2001**.
21. 鍾寶堂; 蔣孝澈, 氧化鈦奈米粒子之表面改質與分散. 國立中央大學化學工程研究所碩士論文 **2005**.
22. Yang, J.; Mei, S.; Ferreira, J. M. F., In situ preparation of weakly flocculated aqueous anatase suspensions by a hydrothermal technique. *Journal of Colloid and Interface Science* **2003**, 260, (1), 82-88.
23. Yang, J.; Mei, S.; Ferreira, J. M. F., Hydrothermal synthesis of TiO₂ nanopowders from tetraalkylammonium hydroxide peptized sols. *Materials Science and Engineering: C* **2001**, 15, (1-2), 183-185.
24. Sasirekha, N.; Rajesh, B.; Chen, Y.-W., Synthesis of TiO₂ sol in a neutral solution using TiCl₄ as a precursor and H₂O₂ as an oxidizing agent. *Thin Solid Films* **2009**, 518, (1), 43-48.
25. Moore, D. T., Gradient-index optics: a review. *Appl Opt* **1980**, 19, (7), 1035-8.
26. Ohtsuka, Y.; Sugano, T., Studies on the light-focusing plastic rod. 14: GRIN rod of CR-39-trifluoroethyl methacrylate copolymer by a vapor-phase transfer process. *Appl Opt* **1983**, 22, (3), 413-7.
27. Liu, J. H.; Liu, H. T.; Cheng, Y. B., Preparation and characterization of gradient refractive index polymer optical rods. *Polymer* **1998**, 39, 5549-5552.

28. Krug, H.; Tiefensee, F.; Oliveira, P. W.; Schmidt, H. K. In *Organic-inorganic composite materials: optical properties of laser-patterned and protective-coated waveguides*, Sol-Gel Optics II, San Diego, CA, USA, 1992; SPIE: San Diego, CA, USA, 1992; pp 448-455.
29. Duijnhoven, F. v.; Bastiaansen, C., Gradient Refractive Index Polymers Produced in a Centrifugal Field. *Advanced Materials* **1999**, 11, (7), 567-570.
30. J.S. Shirk; M. Sandrock; D. Scribner; E. Fleet; R. Stroman; E. Baer; Hiltner, A., Biomimetic Gradient Index (GRIN) Lenses. *FEATURED RESEARCH* **2006**, 53-61.
31. Wang, W.; Fang, J.; Varahramyan, K. In *Controlling nanoparticle distribution in hydrogel by electrophoresis for gradient refractive index lens applications*, Organic Photonic Materials and Devices VII, San Jose, CA, USA, 2005; SPIE: San Jose, CA, USA, 2005; pp 344-351.
32. Niu, G.; Zhang, H.; Song, L.; Cui, X.; Cao, H.; Zheng, Y.; Zhu, S.; Yang, Z.; Yang, H., Thiol/Acrylate-Modified PEO-PPO-PEO Triblocks Used as Reactive and Thermosensitive Copolymers. *Biomacromolecules* **2008**, 9, (10), 2621-2628.
33. Fisher, R. F., The elastic constants of the human lens. *The Journal of Physiology* **1971**, 212, (1), 147-180.
34. Cheng, H.; Ma, J.; Zhao, Z.; Qi, L., Hydrothermal Preparation of Uniform Nanosize Rutile and Anatase Particles. *Chemistry of Materials* **1995**, 7, (4), 663-671.
35. Chau, J. L. H.; Lin, Y.-M.; Li, A.-K.; Su, W.-F.; Chang, K.-S.; Hsu, S. L.-C.; Li, T.-L., Transparent high refractive index nanocomposite thin films. *Materials Letters* **2007**, 61, (14-15), 2908-2910.
36. Larson, I.; Drummond, C. J.; Chan, D. Y. C.; Grieser, F., Direct force measurements between titanium dioxide surfaces. *Journal of the American Chemical Society* **1993**, 115, (25), 11885-11890.
37. Koopmans, S. A.; Terwee, T.; Barkhof, J.; Haitjema, H. J.; Kooijman, A. C., Polymer Refilling of Presbyopic Human Lenses In Vitro Restores the Ability to Undergo Accommodative Changes. *Invest. Ophthalmol. Vis. Sci.* **2003**, 44, (1), 250-257.
38. My Eye World (http://www.myeyeworld.com/files/eye_structure.htm)
39. Royal National Institute for the Blind (<http://www.jwgrundy.co.uk/cataracts.htm>)
40. The Center for Eye Care (<http://lasikbiloxi.com/services/iol/>)
41. Lerman, S., Radiant Energy and the Eye. *MacMillan Publishing Company* **1980**, chap 2
42. Kabanov, A. V.; Batrakova, E. V.; Alakhov, V. Y., Pluronic block copolymers as novel polymer therapeutics for drug and gene delivery. *Journal of Controlled Release* **2002**, 82, (2-3), 189-212.

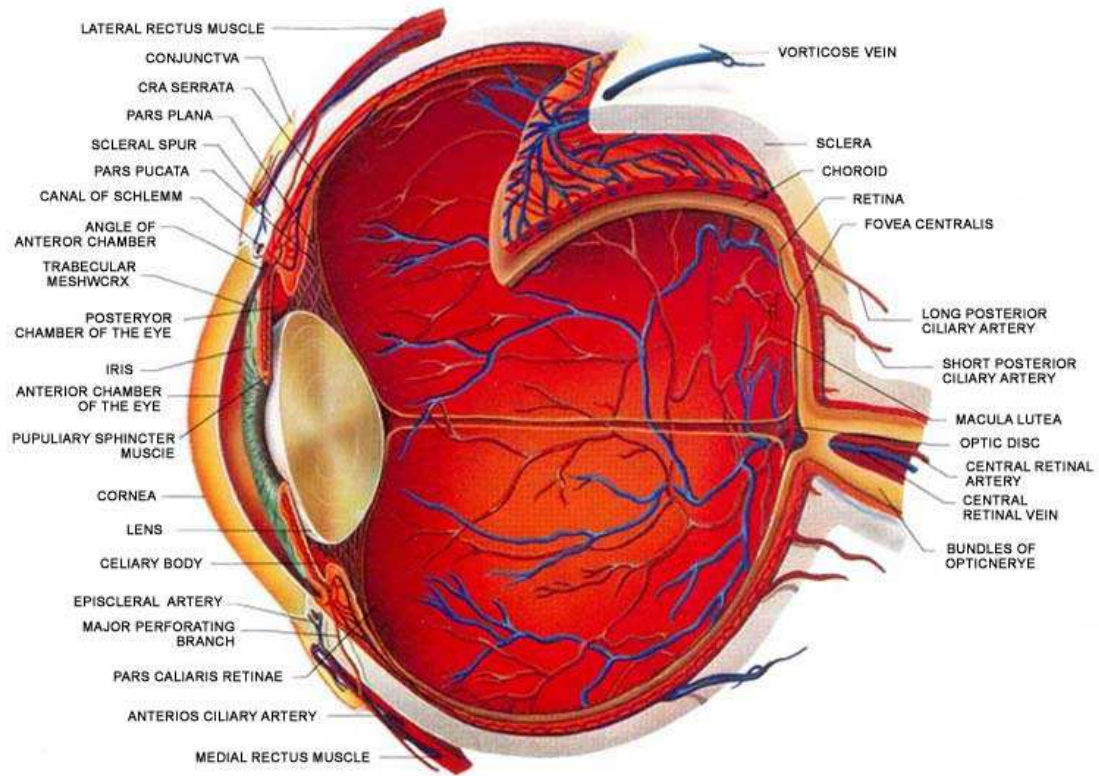


Figure 1. The human eye structure.³⁸



Figure 2. (A) The normal, clear crystalline lens (B) cataract.³⁹

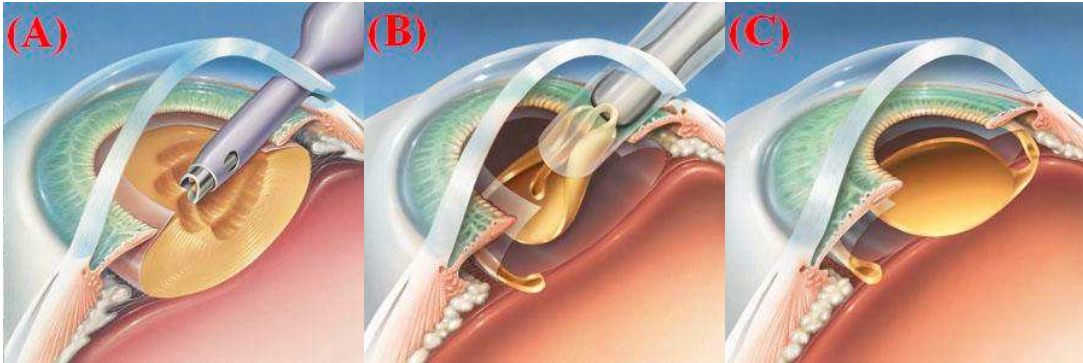


Figure 3. The IOL surgery processes: (A) remove the pathological crystalline lens (B) the IOL inserted to the capsule (C) IOL final position.⁴⁰

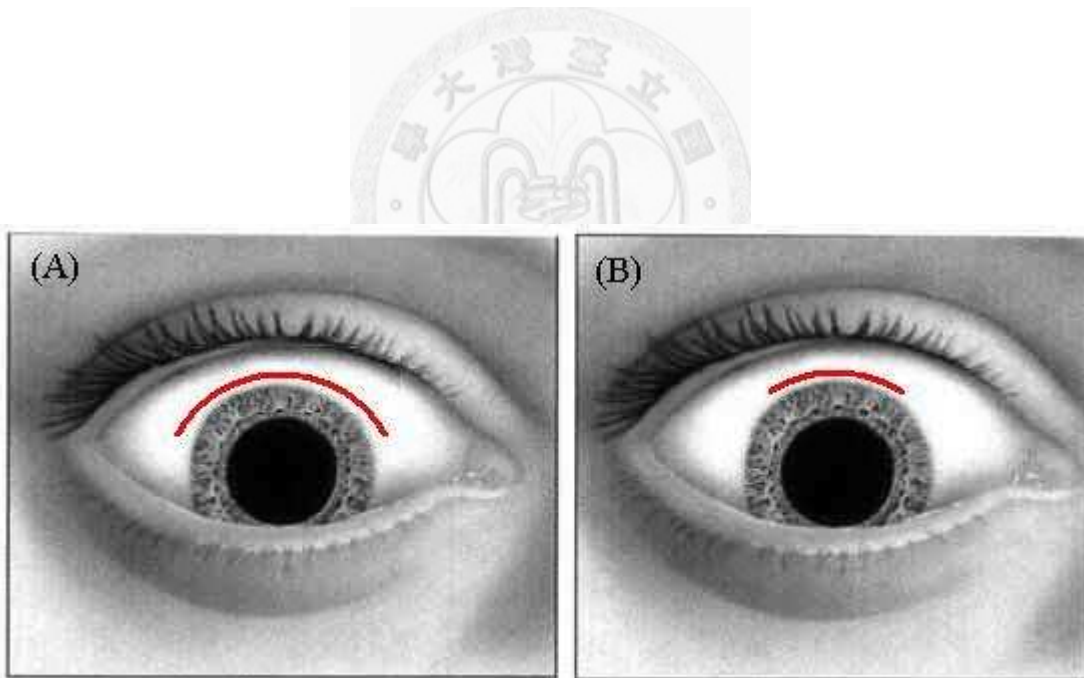


Figure 4. The different wound size according to the transplantation material (A) PMMA (B) soft artificial crystalline lens.

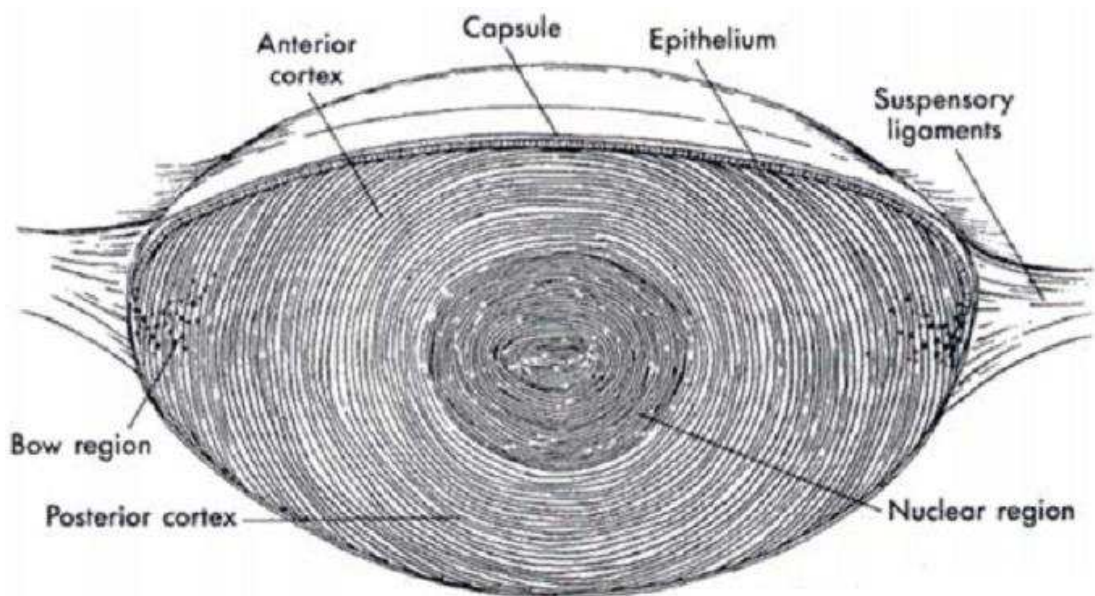


Figure 5. The gradient structure in the human crystalline lens.⁴¹

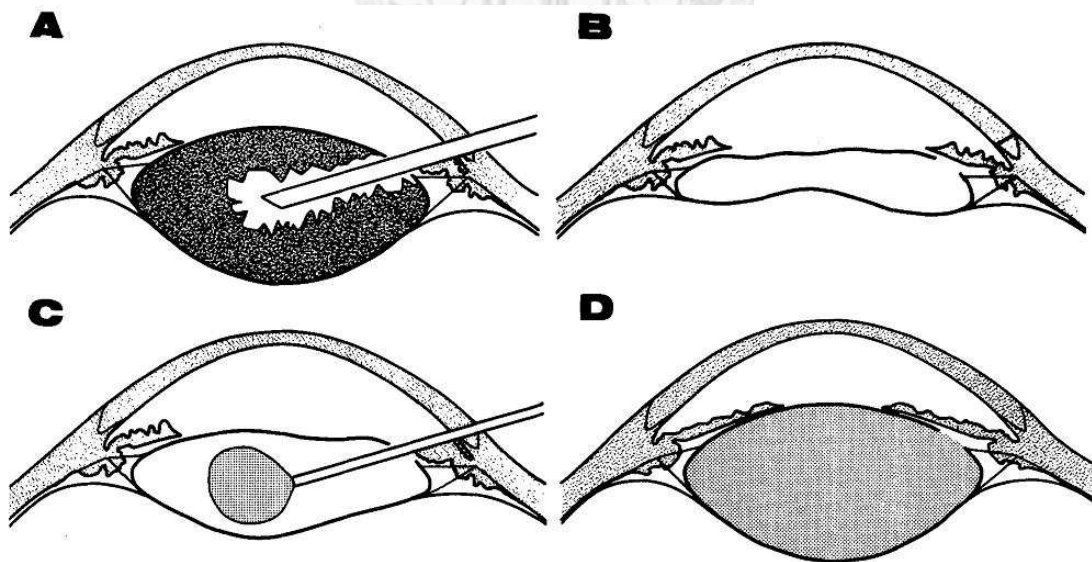


Figure 6. The four steps of the Phaco—Ersatz theory (A) Cataract undergoes emulsification extraction (B) Capsule-zonule-ciliary body framework is maintained (C) Refilling with an ersatz material (D) Ersatz lens designed to preserve accommodation.⁵

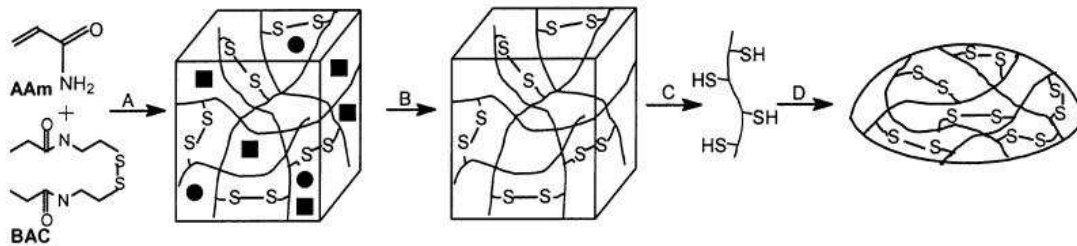


Figure 7. The reversible disulfide copolymer hydrogel system.¹⁴

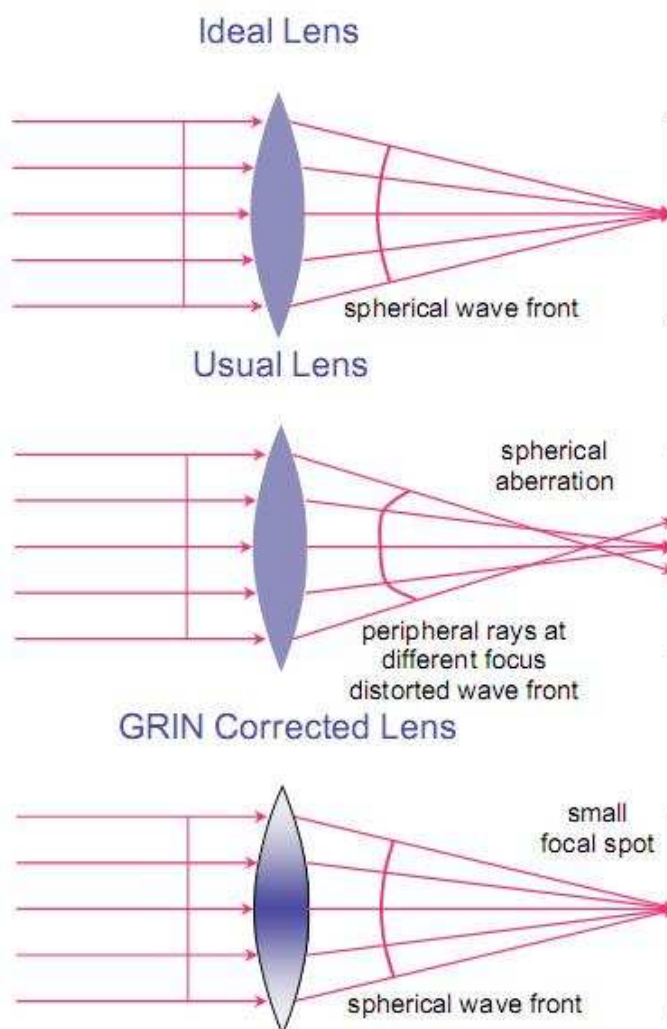


Figure 8. Strategy for spherical aberration correction in a convex lens.³⁰

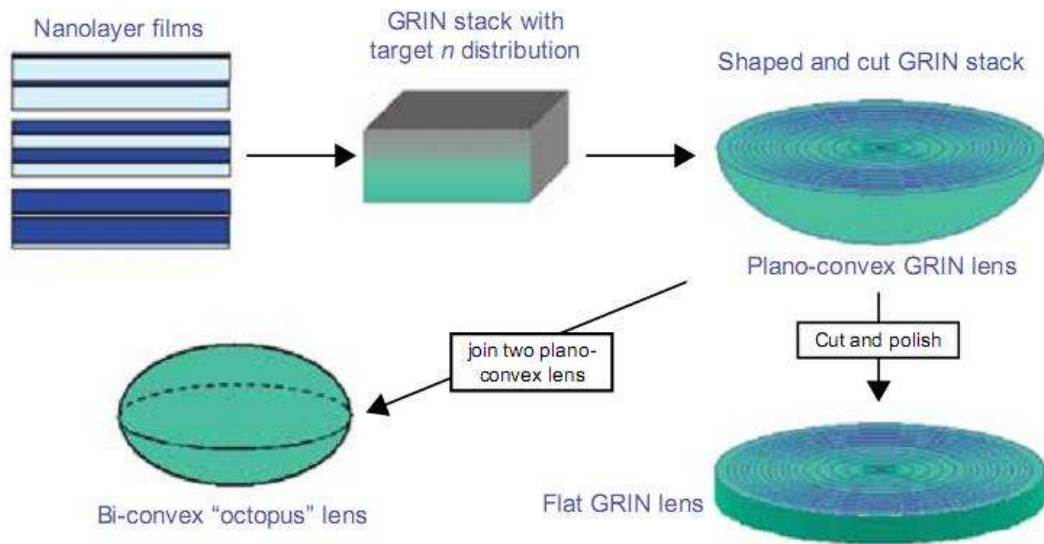


Figure 9. Steps to fabricate a polymer GRIN lens.³⁰

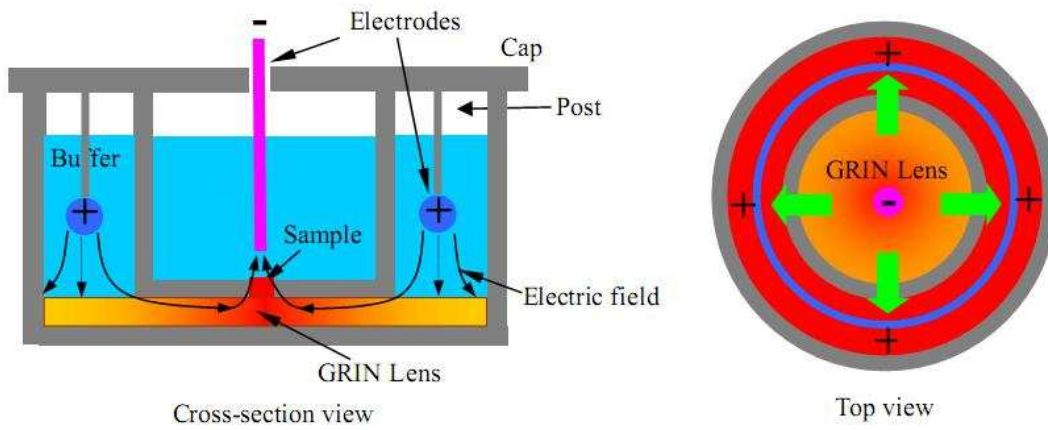
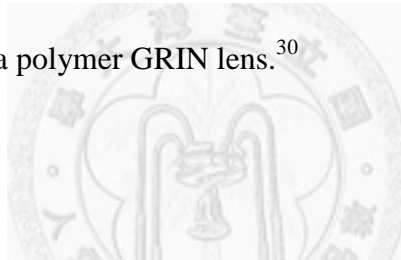


Figure 10. Circular electrophoresis equipment and its working schema.³¹

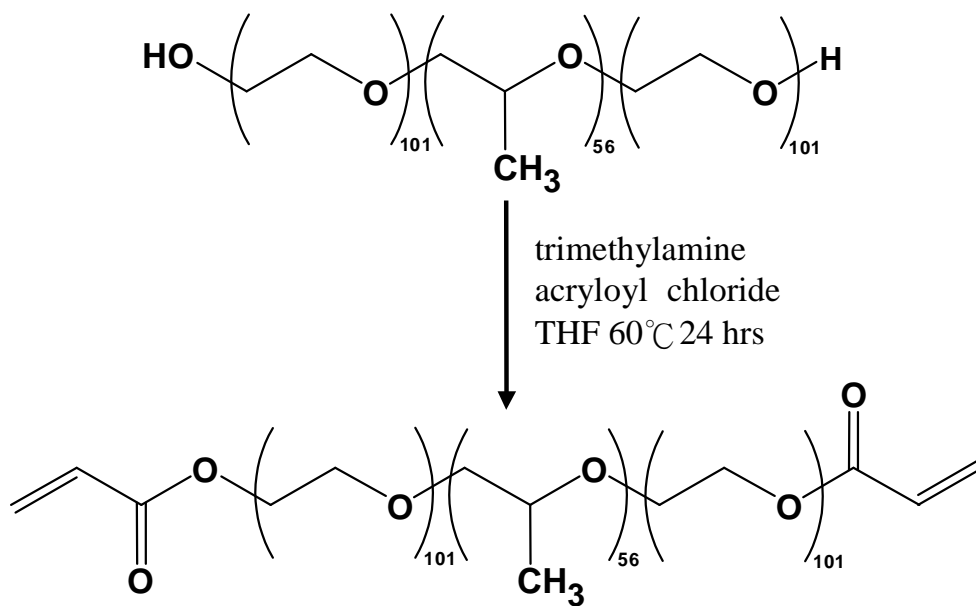


Figure 11. Modification of the terminal groups of poloxamer 407.

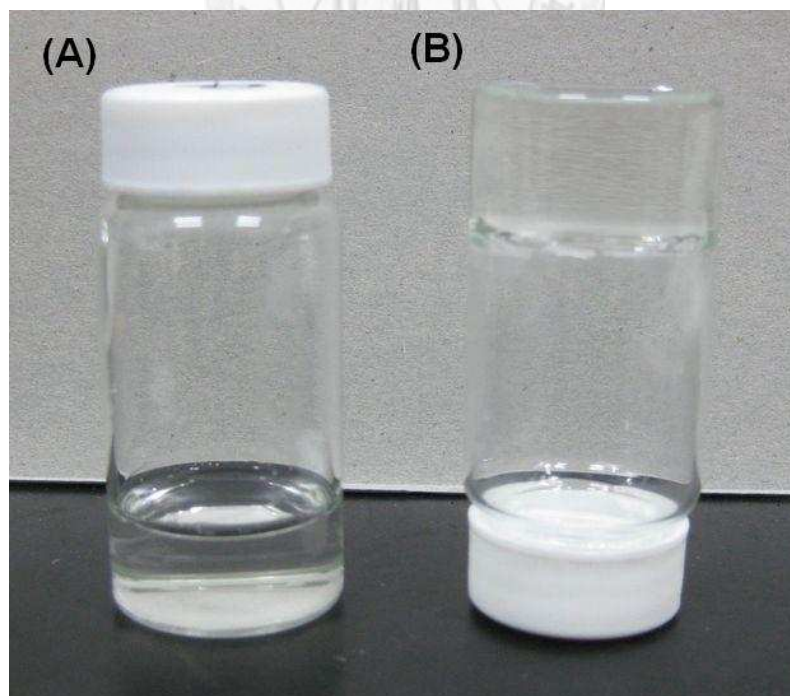


Figure 12. The sol-gel transition phenomenon (A) solution state (B) gelation state.

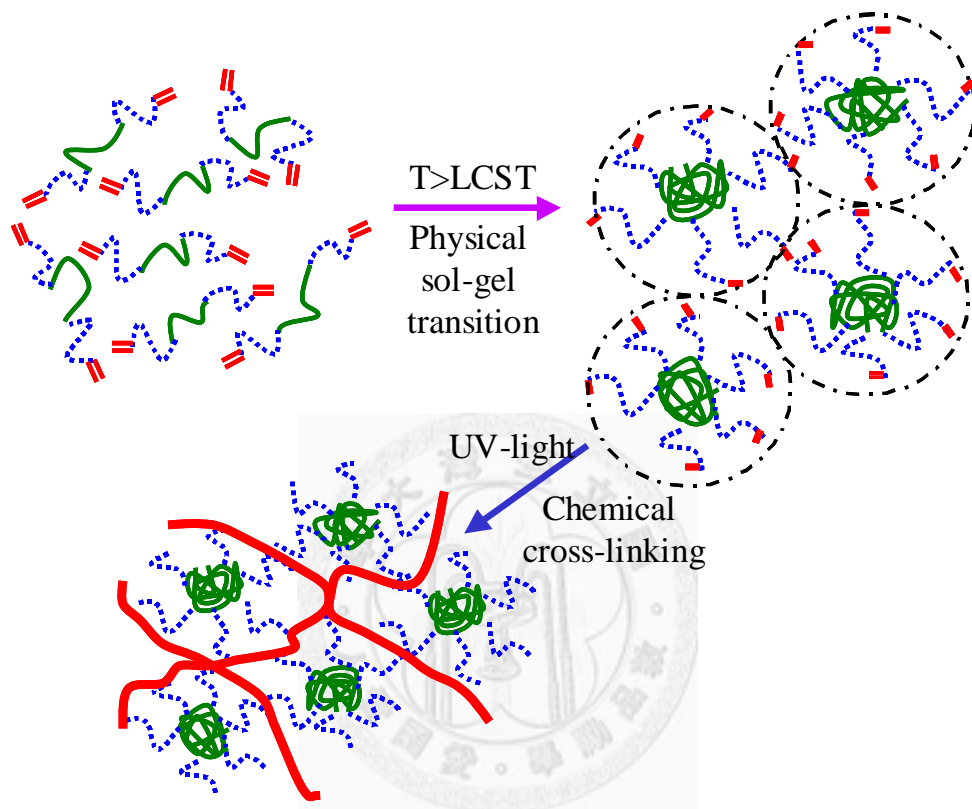


Figure 13. Sol-gel transition and UV-induced photo-cross-linking of diacrylated poloxamer polymer.

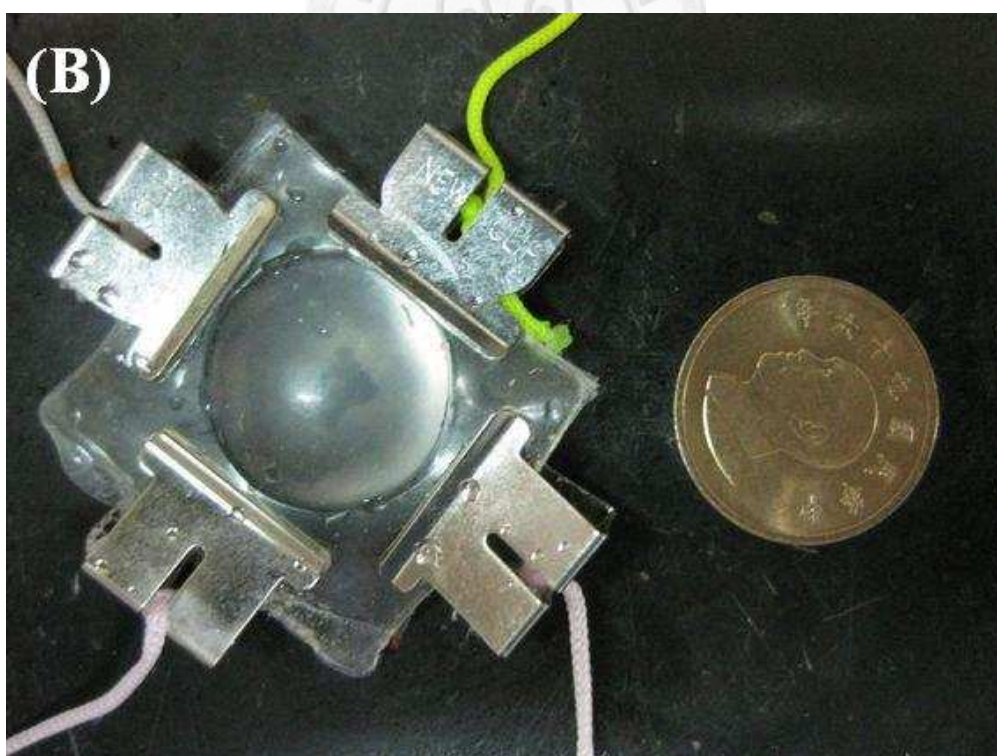
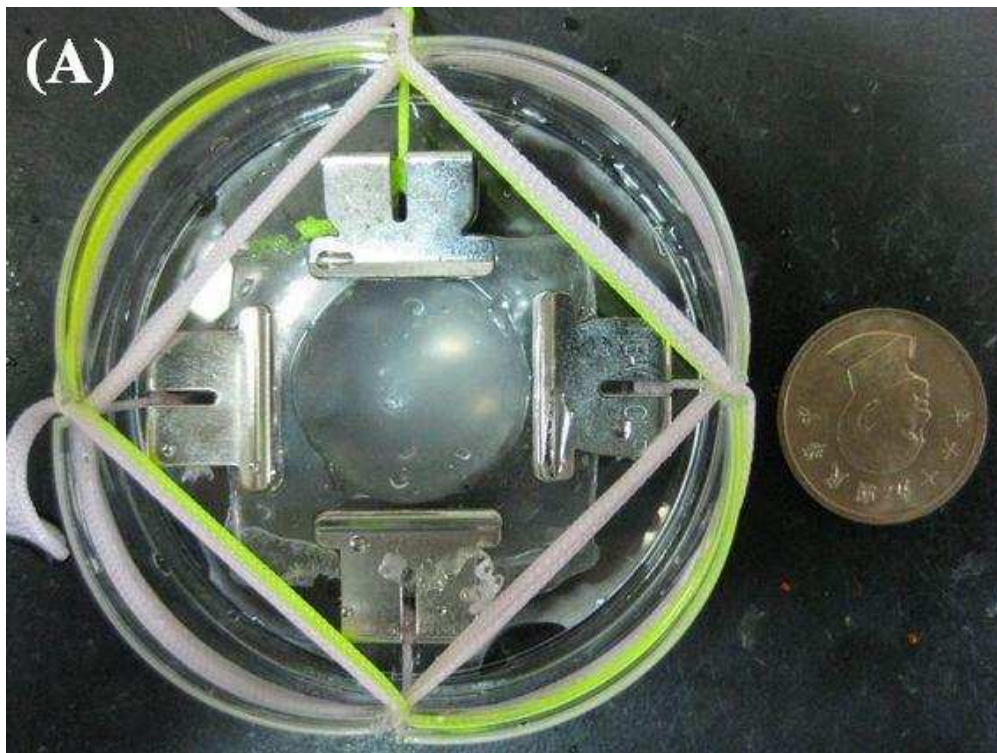


Figure 14. The PDMS capsule filled with poloxamer hydrogel in the (A) stretch (B) unstretch state. (The diameter of the dime is 1.8 cm)

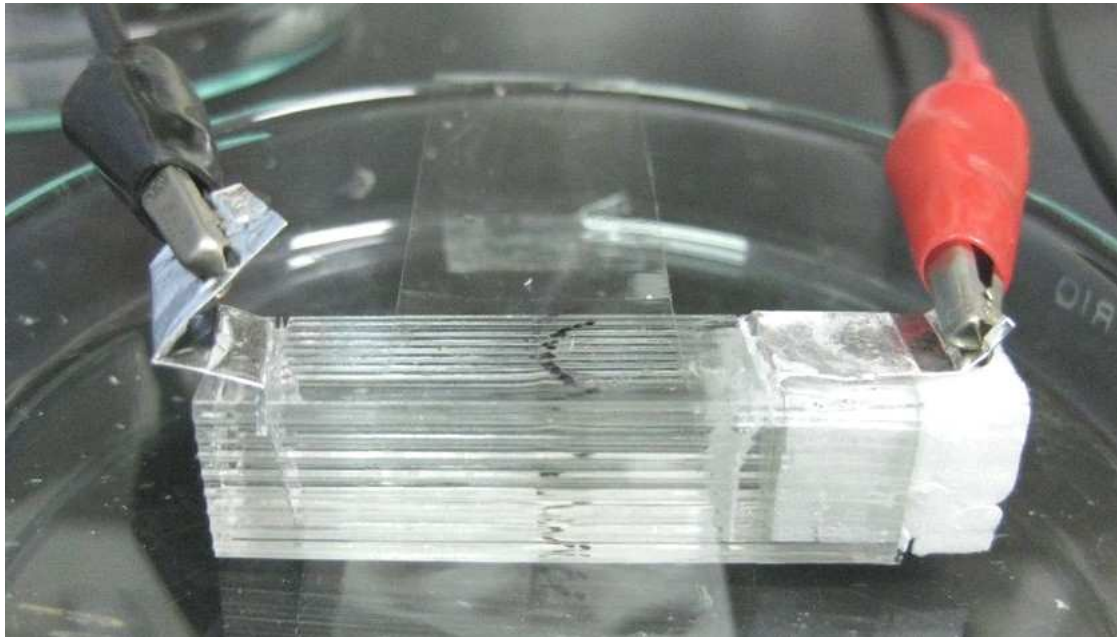


Figure 15. The one-dimensional electric field method using in the experiment

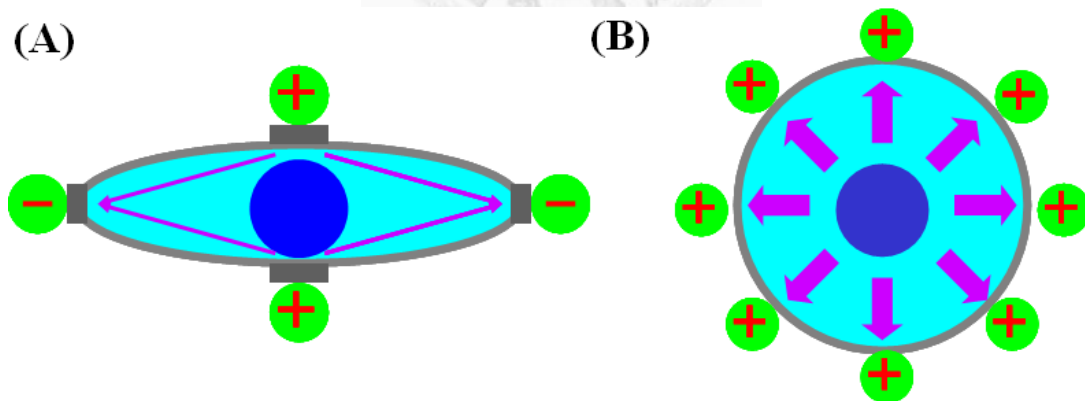


Figure 16. Circular electrophoresis working schema (A) side view (B) top view.

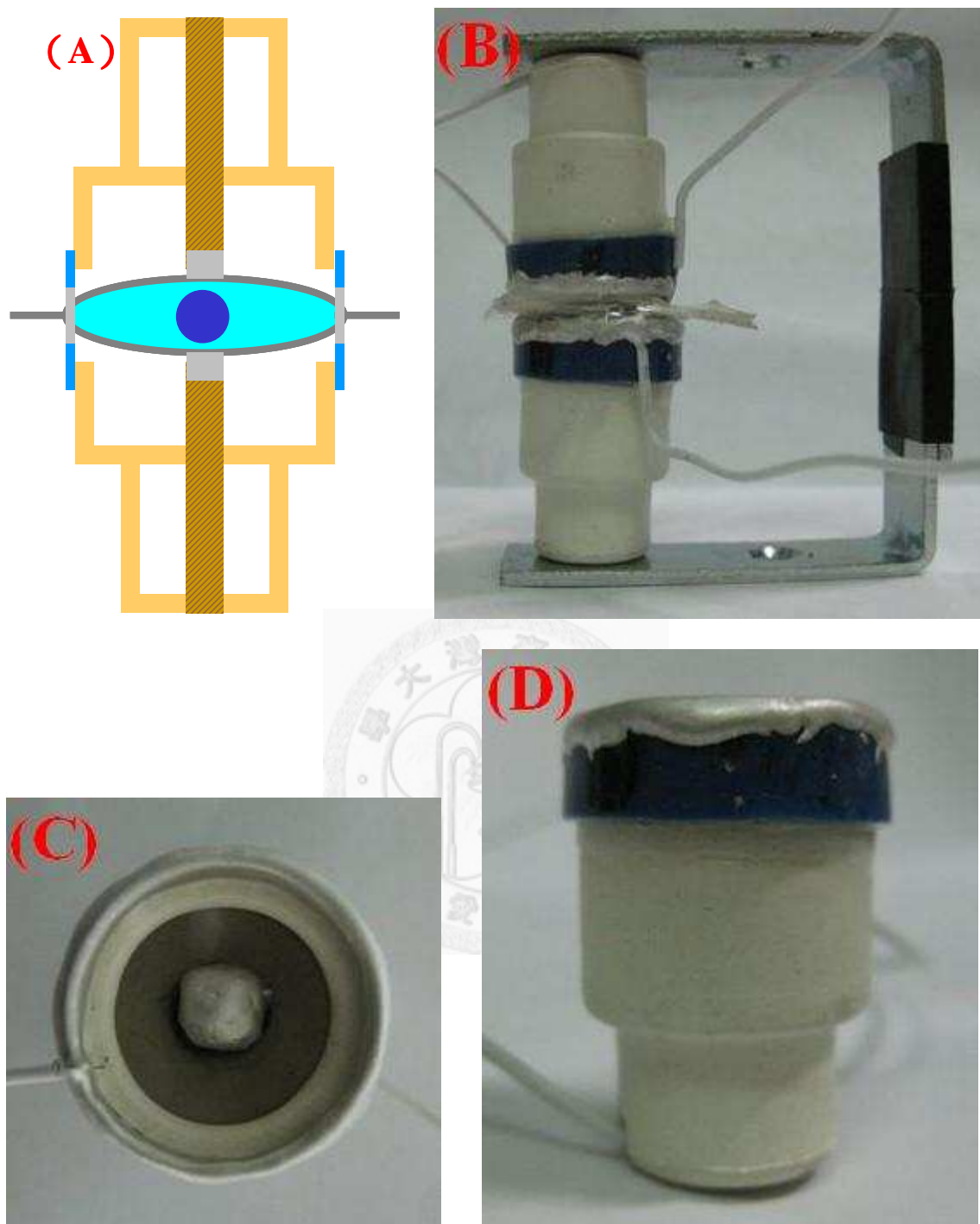


Figure 17. The circular electron in the (A) profile (B) Lateral view (C) Top view (D) Experiment instrument.

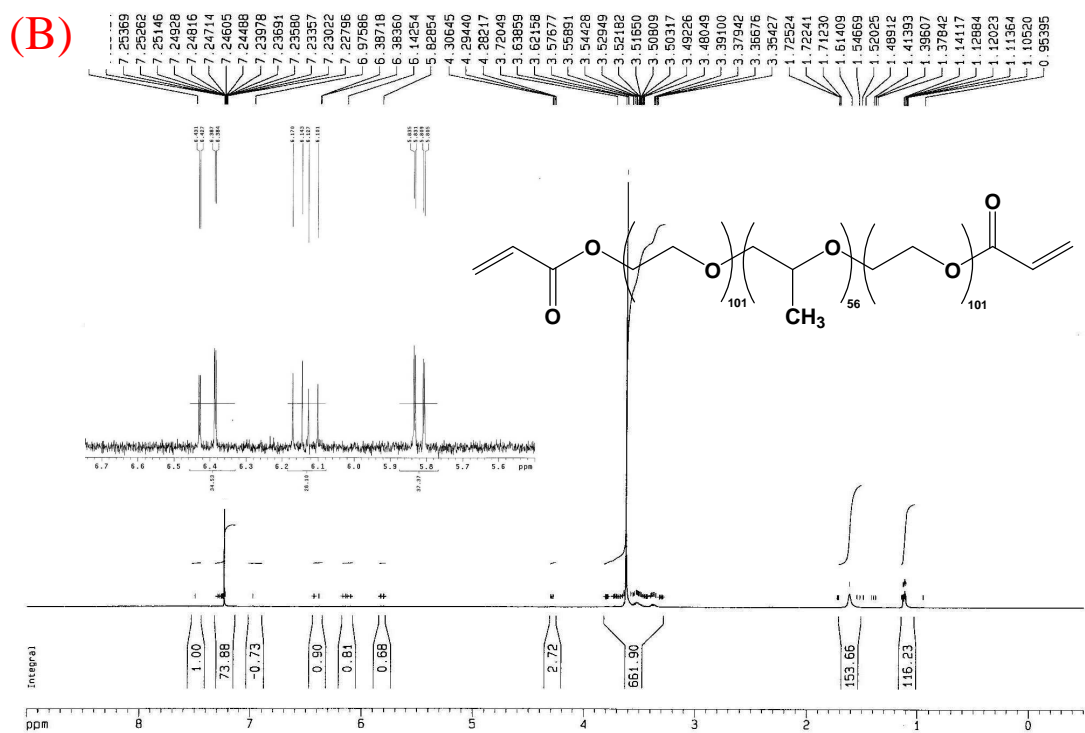
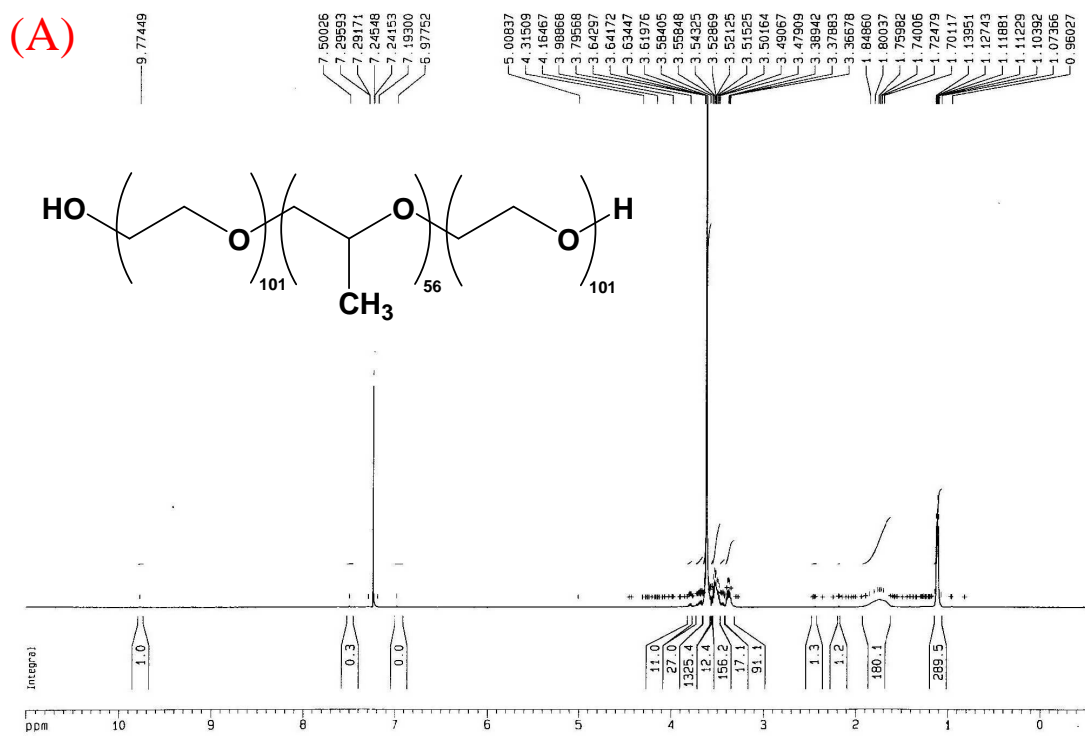


Figure 18. The ^1H -NMR spectrometries of (A) poloxamer 407 and (B) poloxamer 407A.

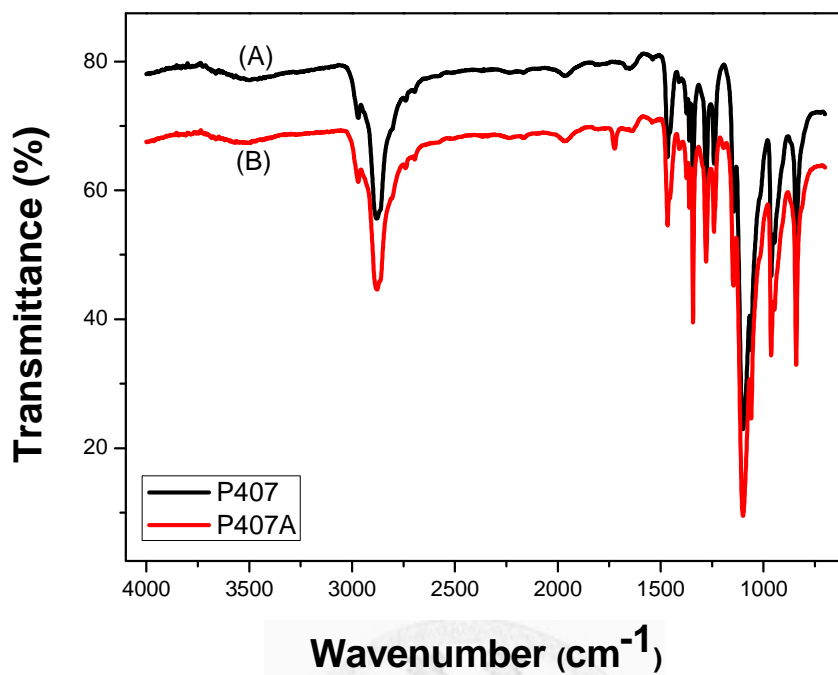


Figure 19. FTIR spectra of (A) poloxamer 407 and (B) poloxamer 407A.

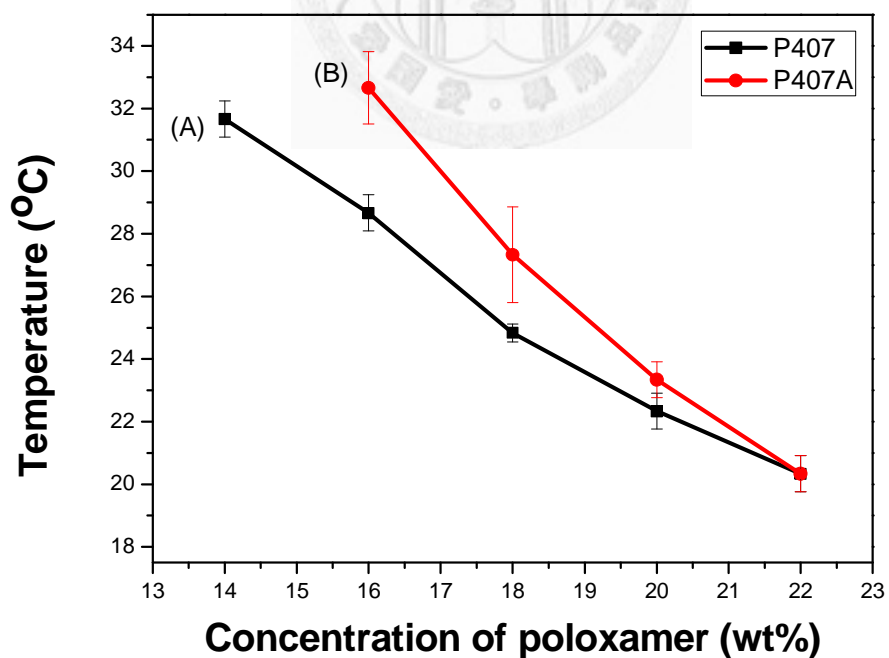


Figure 20. The lower critical sol-gel temperature of (A) poloxamer 407 and (B) poloxamer 407A.

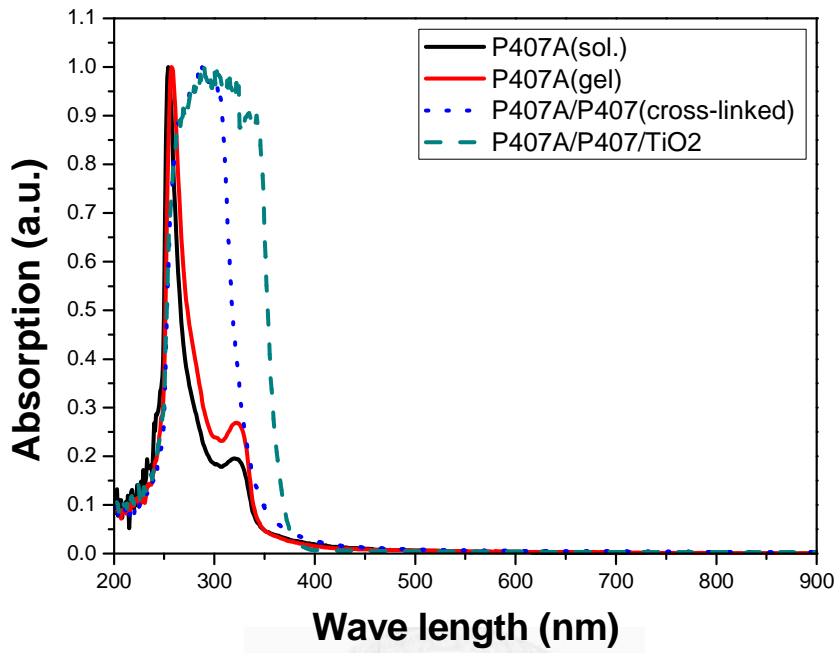


Figure 21. UV-vis absorption of poloxamer hydrogel samples.

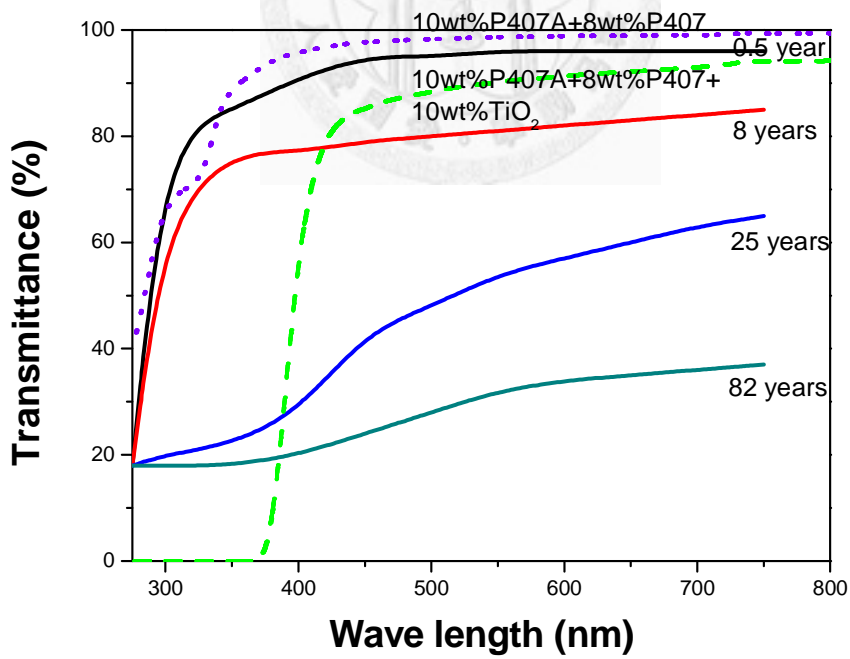


Figure 22. The UV-vis transmittance of Human crystalline lens in different ages⁹ and poloxamer hydrogel samples.

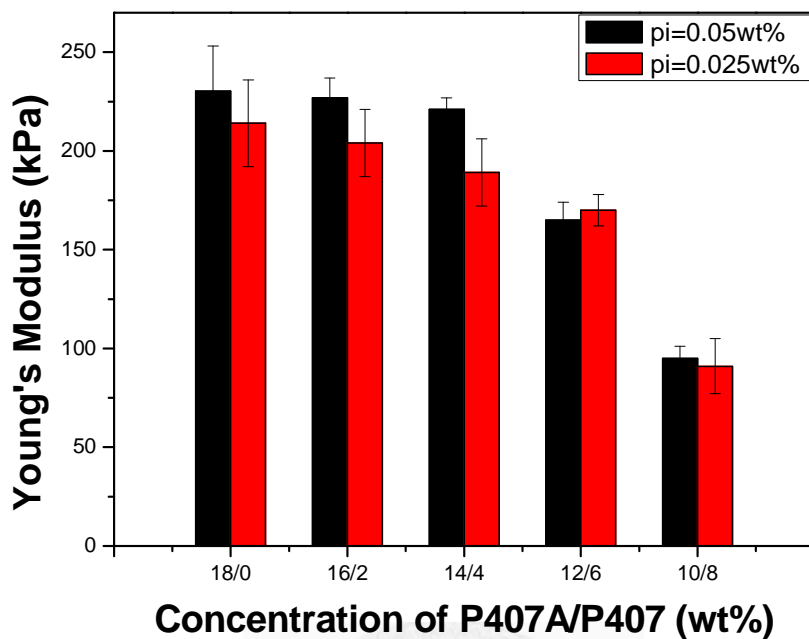


Figure 23. The Young's modulus of the different ratio of poloxamer 407A/407 and concentration of initiator after irradiation for 60s.

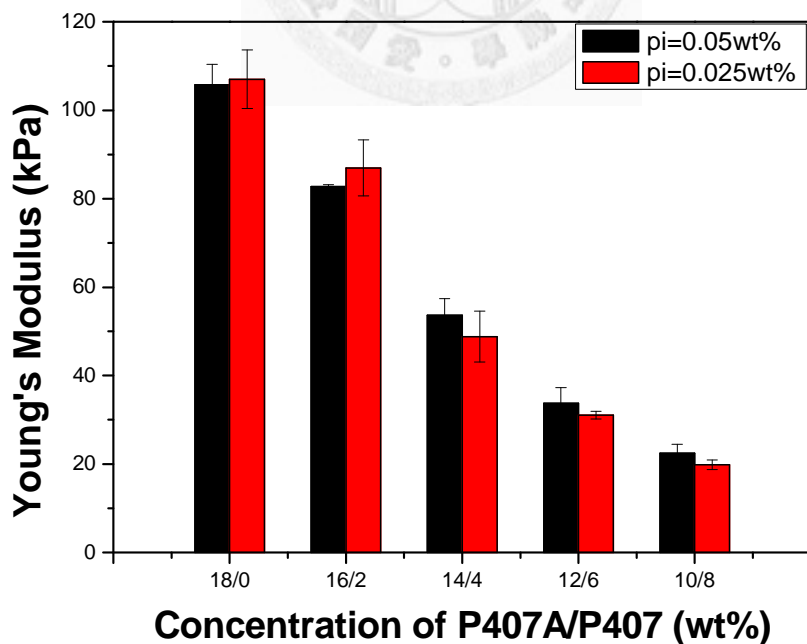


Figure 24. The Young's modulus of the different ratio of poloxamer 407A/407 and concentration of initiator after irradiation for 30s.

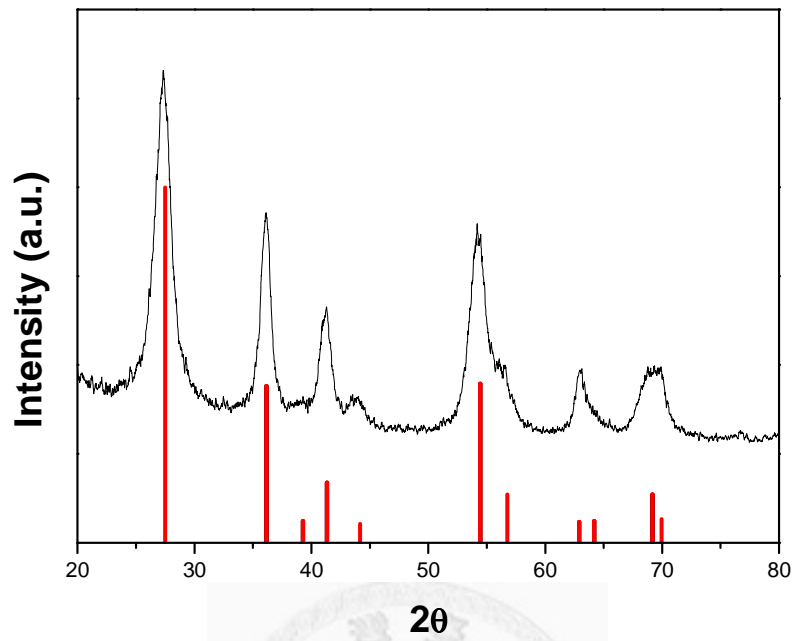


Figure 25. XRD patterns of titanium dioxide nano particles (lines: rutile phase JCPDS no. 89-4920).

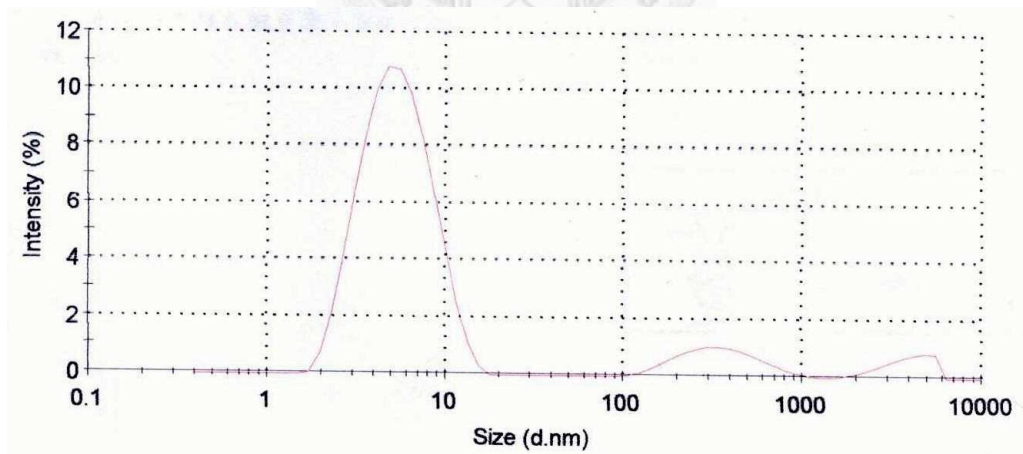


Figure 26. The particle diameter distribution of titanium dioxide nanoparticles.

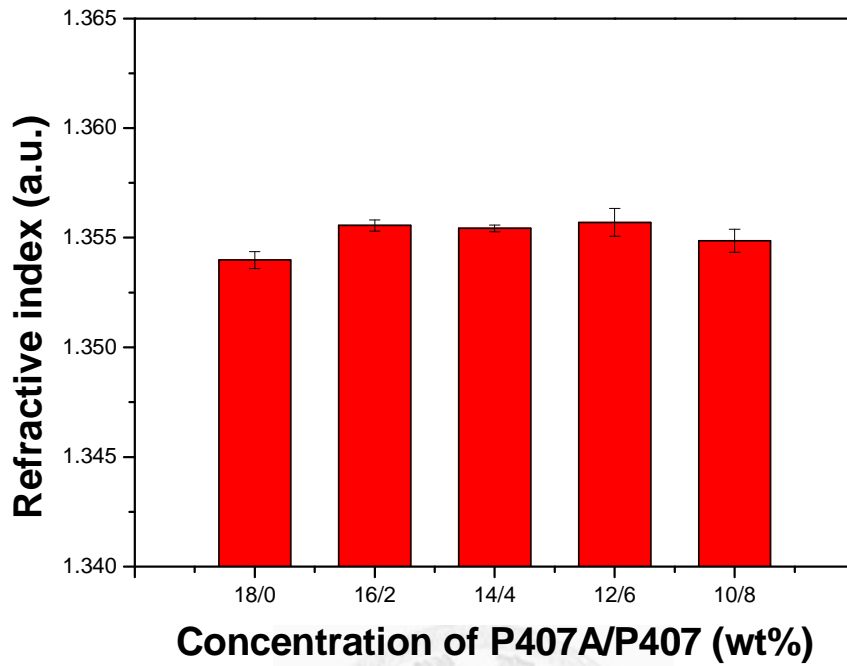


Figure 27. The refractive index of the different ratio of poloxamer 407 and 407A.

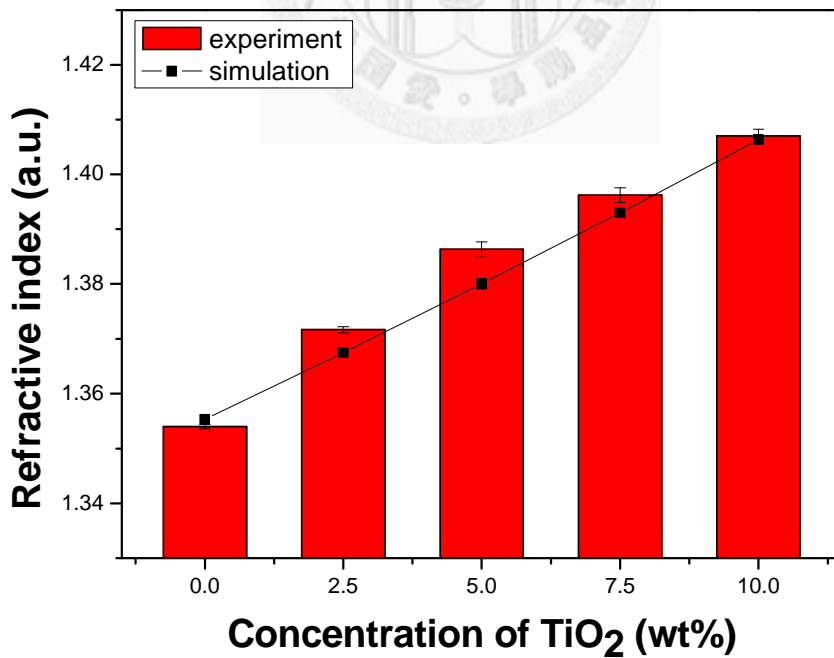


Figure 28. The refractive index of poloxamer hydrogel containing different concentration of titanium dioxide nanoparticles.

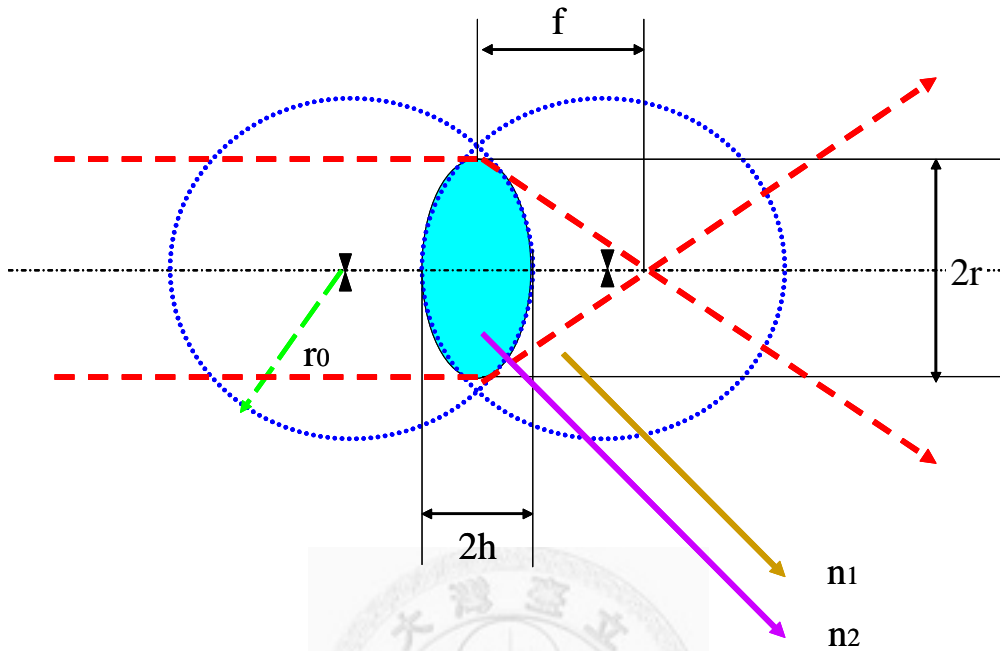


Figure 29. The lensmaker's equation model.

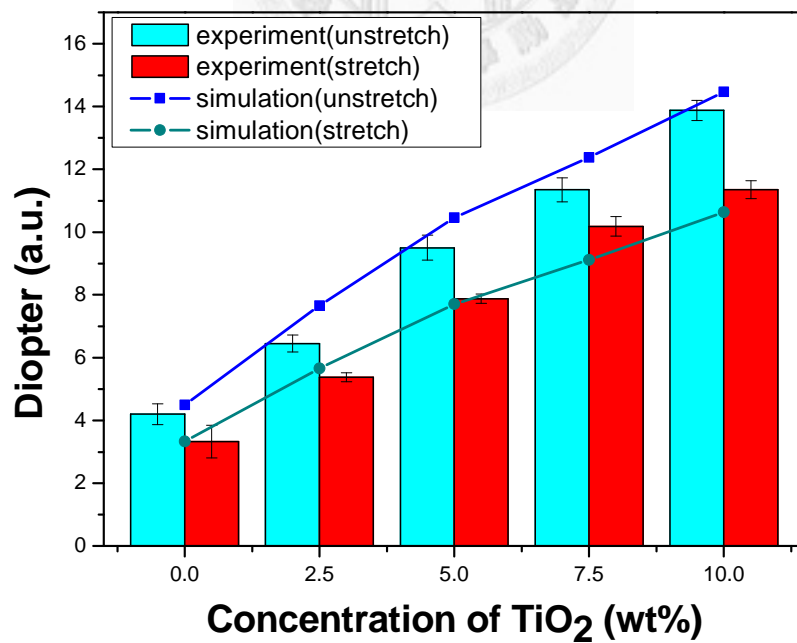


Figure 30. The stretch and unstretch focal length changes according to the different concentration of titanium dioxide nanoparticles.

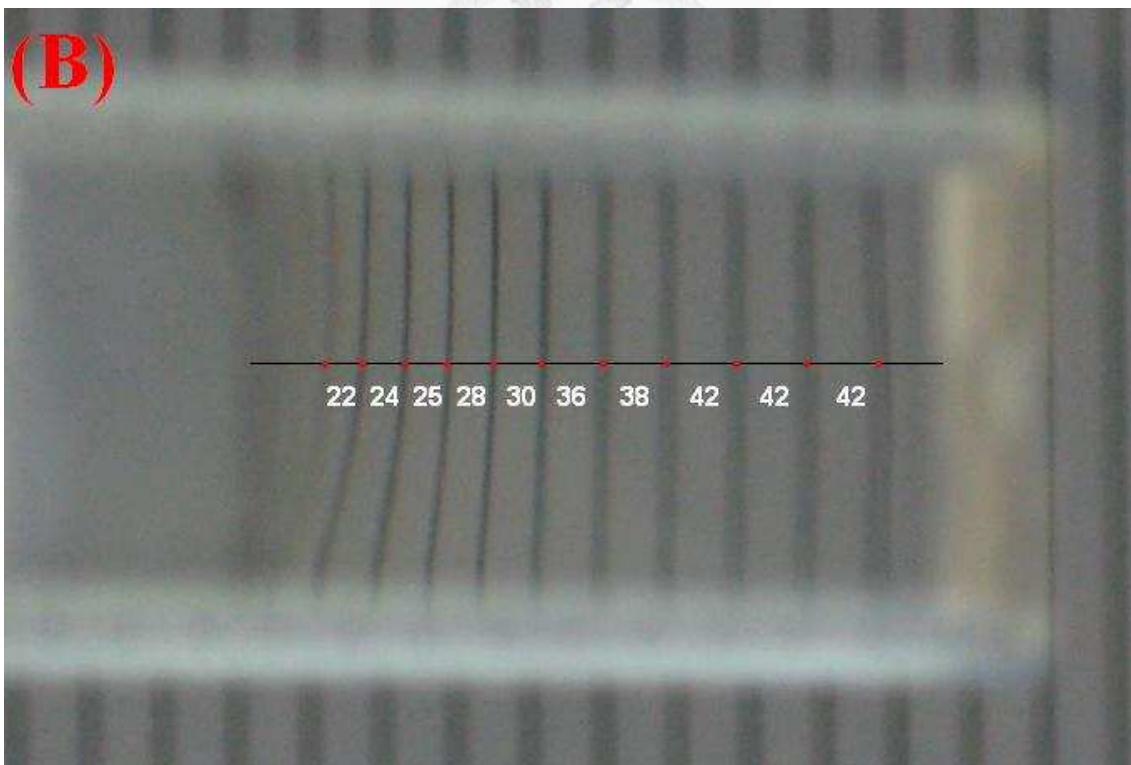
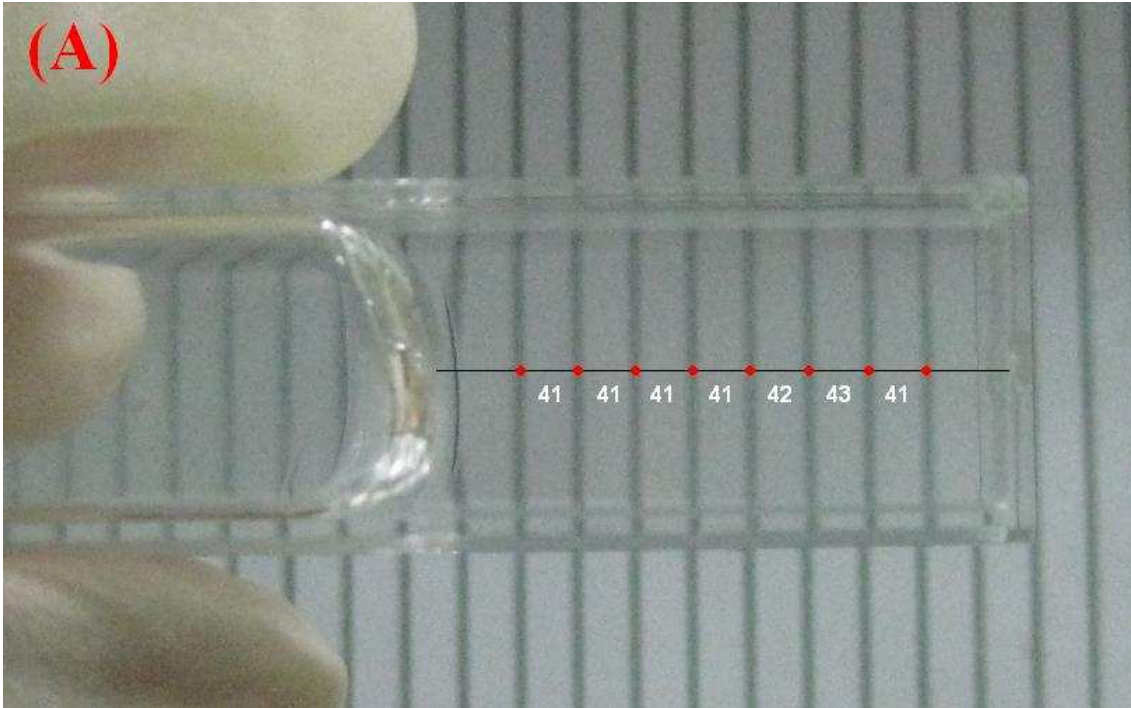


Figure 31. (A) The distance of the lines through poloxamer hydrogel are equal before interface moving method (B) The distance of the lines through poloxamer hydrogel are decreasing after the interface moving method.



Figure 32. Poloxamer hydrogel bulk moving phenomenon in the centrifuge method.

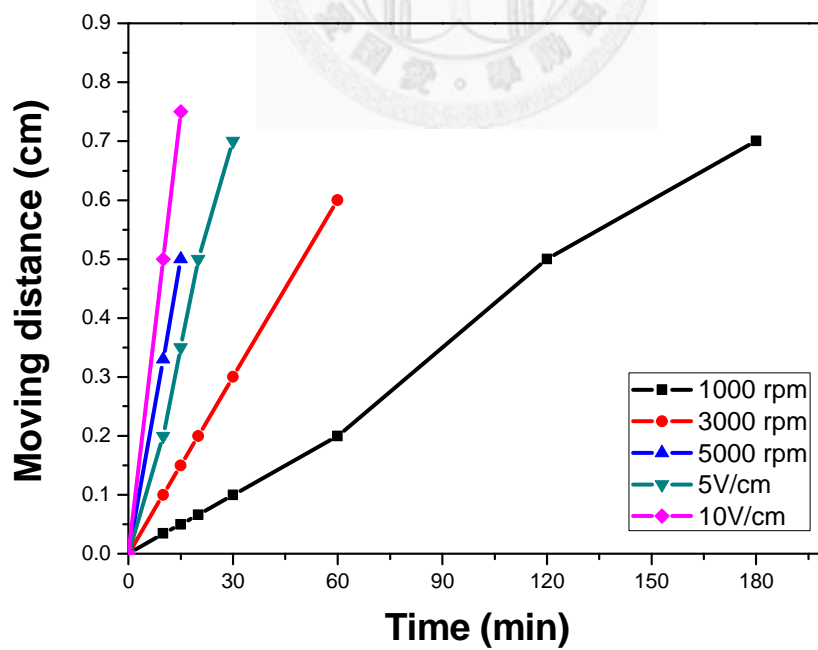


Figure 33. The moving rate with the different methods.

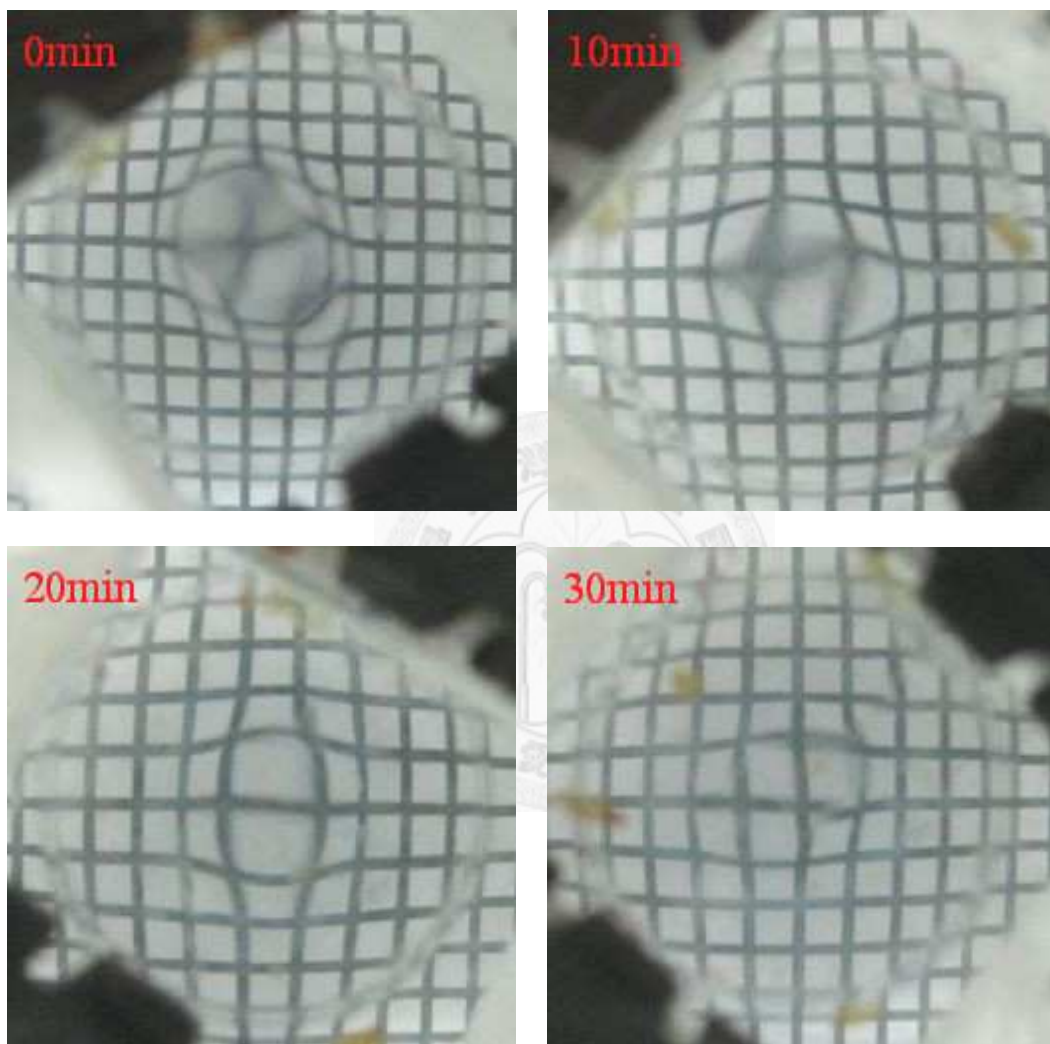


Figure 34. The change of image quality according to the different times of electron field at 5V/cm.

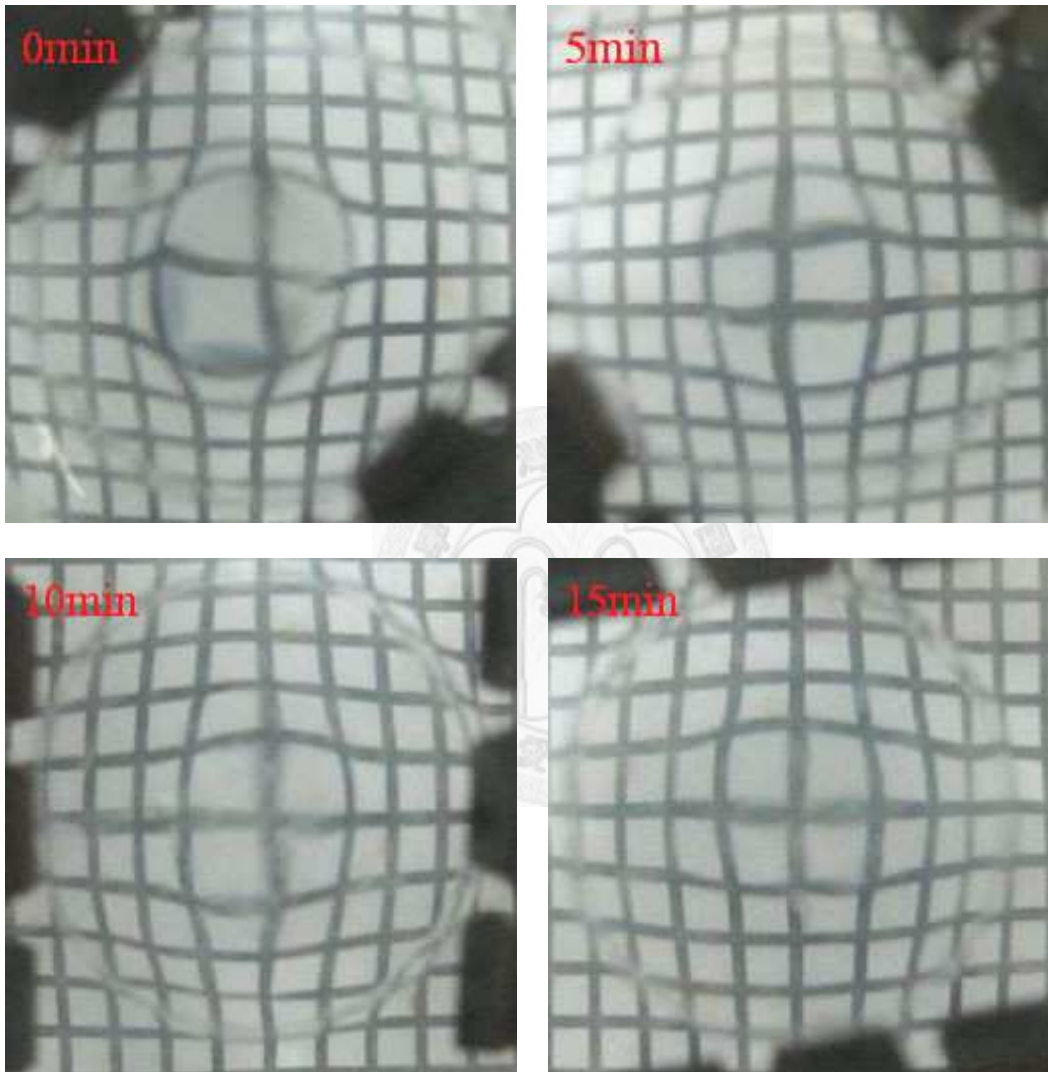


Figure 35. The change of image quality according to the different times of electron field at 10V/cm.

Table 1. Physical properties material of the human lens contents and hypothetical values of an ideal ersatz⁵

Parameter	Value
Refractive index	1.405±0.002
Dispersion coefficient	56.2±2
Transmission factor	0.95±0.05
Specific density	1.06±0.03
H ₂ O absorption	0 (hydrophilic)
Elastic modulus	2X10 ³ nm ⁻² (accuracy unknown)
Elongation limit	50% (accuracy unknown)
Anelastic coefficient	0.5 (theoretical valve)

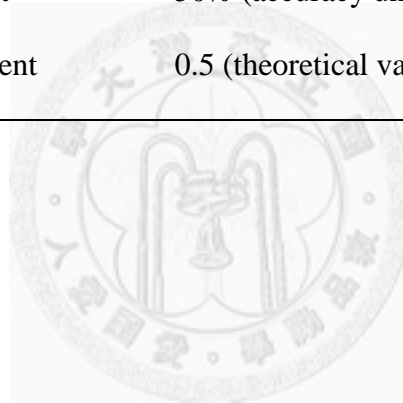


Table 2. Physicochemical characteristics of Pluronic[®] block copolymers⁴²

Copolymer	MW	Average no. of EO units(x)	Average no. of PO units(y)	HLB	Cloud point in 1% aqueous solution (°C)	CMC (M)
L35	1900	21.59	16.38	19	73	5.3X10 ⁻³
L43	1850	12.61	22.33	12	42	2.2 X10 ⁻³
L44	2200	20.00	22.76	16	65	3.6 X10 ⁻³
L61	2000	4.55	31.03	3	24	1.1 X10 ⁻⁴
L62	2500	11.36	34.48	7	32	4.0 X10 ⁻⁴
L64	2900	26.36	30.00	15	58	4.8 X10 ⁻⁴
F68	8400	152.73	28.97	29	>100	4.8 X10 ⁻⁴
L81	2750	6.25	42.67	2	20	2.3 X10 ⁻⁵
P84	4200	38.18	43.45	14	74	7.1 X10 ⁻⁵
P85	4600	52.27	39.66	16	85	6.5 X10 ⁻⁵
F87	7700	122.50	39.83	24	>100	9.1 X10 ⁻⁵
F88	11400	207.27	39.31	28	>100	2.5 X10 ⁻⁴
L92	3650	16.59	50.34	6	26	8.8 X10 ⁻⁵
F98	13000	236.36	44.83	28	>100	7.7 X10 ⁻⁵
L101	3800	8.64	58.97	1	15	2.1 X10 ⁻⁶
P103	4950	33.75	59.74	9	86	6.1 X10 ⁻⁶
P104	5900	53.64	61.03	13	81	3.4 X10 ⁻⁶
P105	6500	73.86	56.03	15	91	6.2 X10 ⁻⁶
F108	14600	265.45	50.34	27	>100	2.2 X10 ⁻⁵
L121	4400	10.00	68.28	1	14	1.0 X10 ⁻⁶
P123	5750	39.2	69.40	8	90	4.4 X10 ⁻⁶
F127	12600	200.45	65.17	22	>100	2.8 X10 ⁻⁶

Table 3. The concentration of poloxamer hydrogel in the sol-gel experiment

	P407 or P407A(g)	H ₂ O(g)
16 wt%	0.8	4.2
18 wt%	0.9	4.1
20 wt%	1.0	4.0
22 wt%	1.1	3.9

Table 4. The concentration of poloxamer hydrogel in the Mechanical properties test

	Poloxamer 407A(g)	Poloxamer 407(g)	H ₂ O(g)	Photo initiator(mg)	Irradiation time(s)
18/0	0.9	0.0	4.1	2.50	60
16/2	0.8	0.1	4.1	2.50	60
14/4	0.7	0.2	4.1	2.50	60
12/6	0.6	0.3	4.1	2.50	60
10/8	0.5	0.4	4.1	2.50	60
18/0	0.9	0.0	4.1	1.25	60
16/2	0.8	0.1	4.1	1.25	60
14/4	0.7	0.2	4.1	1.25	60
12/6	0.6	0.3	4.1	1.25	60
10/8	0.5	0.4	4.1	1.25	60
18/0	0.9	0.0	4.1	2.50	30
16/2	0.8	0.1	4.1	2.50	30
14/4	0.7	0.2	4.1	2.50	30
12/6	0.6	0.3	4.1	2.50	30
10/8	0.5	0.4	4.1	2.50	30
18/0	0.9	0.0	4.1	1.25	30
16/2	0.8	0.1	4.1	1.25	30
14/4	0.7	0.2	4.1	1.25	30
12/6	0.6	0.3	4.1	1.25	30
10/8	0.5	0.4	4.1	1.25	30

Table 5. Composition of the prepared poloxamer hydrogel containing titanium dioxide nanoparticles

TiO ₂ (wt%)	Ti(OH) ₄ (g)	TiO ₂ (g)	HCl (ml)	H ₂ O (g)	P407 (g)	P407A (g)	Photo initiator (mg)	Total (g)
0.0	0.0	0.0	0.0	4.10	0.40	0.50	2.5	5.0
2.5	1.0	0.2	0.3	5.26	0.64	0.80	4.0	8.0
5.0	1.0	0.2	0.3	1.98	0.32	0.40	2.0	4.0
7.5	1.0	0.2	0.3	0.89	0.217	0.27	1.4	2.7
10.0	1.0	0.2	0.3	0.34	0.16	0.20	1.0	2.0